Part A3 – The Electromagnetic Torus as a Model of the Electron

Franc Rozman

Abstract

This article investigates the electron as a stable, energy-saturated electromagnetic torus consisting of three dynamically coupled fields: electric E, magnetic B, and motion-related P. The P field introduces an independent inertial response and participates in the periodic energy-transfer sequence E → P → B → P → E, supporting the coherent internal dynamics of the structure.

A simplified three-field model yields a collective propagation velocity approaching 0.8165c. By relating the fundamental closed mode (n = 1) to the characteristic period associated with the electron rest energy, a major toroidal radius of approximately 0.315 pm is obtained.

The proposed geometry provides a common framework for investigating electron angular momentum and magnetic moment. An illustrative field-energy distribution yields a mean axial angular momentum of approximately 0.5006ħ, while an effective current distribution concentrated toward the outer region of the torus can reproduce the characteristic scale of the electron magnetic moment.

Electric charge is examined as an effective property of the external electric field generated by periodic internal electromagnetic processes. The model establishes a quantitative relationship between the internal electric-field amplitude, the temporal transmission window, and the equivalent charge. The measured electron charge is used to determine the required field amplitude.

Together, these results establish quantitative connections between toroidal geometry, collective field inertia, and several fundamental properties of the electron. The proposed model offers a unified electromagnetic framework for investigating the electron as a coherent field structure and provides a foundation for further development of the theory.

1. Introduction

The electron is characterized by a remarkable combination of physical properties: a precisely defined rest energy, a stable electric charge, intrinsic angular momentum, and a magnetic moment. These properties are accurately described within quantum theory, where the electron is treated as an elementary spin-1/2 particle. However, this description does not assign the electron a resolved internal electromagnetic structure.

The present article investigates a different possibility: that the electron may correspond to a stable, energy-saturated electromagnetic torus whose internal dynamics give rise to several of its observed properties.

The electromagnetic supertorus is a closed configuration characterized by two geometrical dimensions: the major radius R and the minor radius a. Its internal structure consists of mutually coupled electric E, magnetic B, and motion-related P fields. The three fields participate in a continuous exchange of energy while maintaining a coherent spatial configuration.

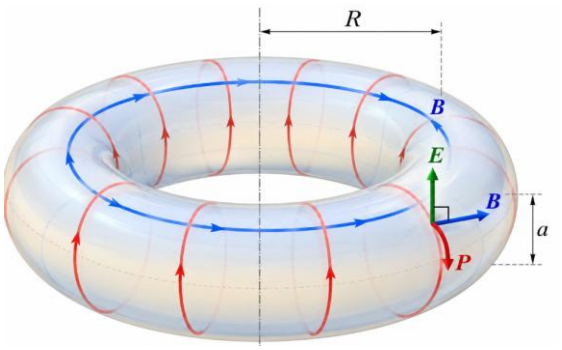


Figure 1. *General geometry of the proposed electromagnetic torus identified as a candidate model of the electron. The structure is characterized by the major radius R, the minor radius a, and the coupled field components E, B, and P.*

The central hypothesis is that an electron corresponds to the fundamental closed mode of such a structure, with one complete phase cycle around the major circumference n = 1. In this state, the electromagnetic torus has reached a configuration in which further geometrical expansion and energy redistribution are constrained by its internal field dynamics.

An essential feature of the proposed structure is the periodic exchange of energy between the three fields. Unlike a freely propagating electromagnetic wave, the electron supertorus is assumed to support a phase-shifted internal oscillation in which energy passes through the sequence

E → P → B → P → E.

The P field is assigned an independent inertial response. It participates in the transfer of energy between the electric and magnetic components and influences the collective propagation of the coupled structure. Consequently, the common electromagnetic pattern may advance around the major circumference at a velocity lower than the speed of light, even though the local electromagnetic processes remain governed by their own characteristic dynamics.

This distinction provides a possible connection between the internal inertia of the supertorus and its characteristic oscillation period. A simplified model with comparable inertial contributions from E, B, and P yields a collective propagation velocity of approximately 0.816c under strong coupling. The resulting period is of the same order as the characteristic period associated with the electron rest energy.

The model also offers a geometrical framework for investigating angular momentum and magnetic moment. Electromagnetic energy and effective electric-current distributions need not occupy identical regions of the toroidal cross-section. Their different radial distributions and directions of circulation may therefore produce different contributions to angular momentum and magnetic moment. This distinction is central to examining whether a single torus configuration can reproduce the

experimentally known values of both quantities.

A further aspect concerns electric charge. In the proposed model, the external electric field is examined as a possible consequence of the asymmetric organization of internal electromagnetic oscillations. Electric fields directed toward the center of the toroidal cross-section are encounter opposing field contributions and the response of the P field. Conversely, outward-directed electric components may contribute to the surrounding field. Their spatial and temporal superposition can produce a persistent average external electric field, even when the underlying local dynamics are impulsive.

The present investigation builds on the preceding development of electromagnetic tori. Part A1 examined their field structure, internal energy balance, and stability conditions, while Part A2 investigated the merging of toroidal structures and the redistribution of energy during structural evolution. The present Part A3 focuses on the resulting saturated state and its possible identification with the electron.

The objective is not to reconstruct every detail of the internal electromagnetic dynamics. Instead, the analysis seeks a consistent connection between a limited set of structural assumptions and the principal measured properties of the electron. Particular attention is given to the relationships among toroidal geometry, energy, characteristic period, angular momentum, electric charge, and magnetic moment.

A successful structural model must ultimately satisfy these constraints within one and the same configuration. The following sections therefore develop a simplified quantitative description of the saturated supertorus and compare its consequences with the known physical properties of the electron. [2], [5], [7], [8]

2. Electron Properties and Model Constraints

The electron provides an exceptionally well-defined physical reference for investigating the proposed electromagnetic torus. Its rest mass, electric charge, intrinsic angular momentum, and magnetic moment are known with high experimental precision. These quantities establish a set of constraints that any proposed structural model of the electron must satisfy.

In the present model, the electron is represented by an energy-saturated electromagnetic torus consisting of three mutually coupled fields: E, B, and P. Rather than treating the observed properties of the electron as unrelated characteristics, the objective is to examine whether they can be associated with the geometry and internal dynamics of a single stable structure.

2.1 Electron Rest Mass and Energy

The electron rest mass is approximately

$$m_e = 9.10938 \times 10^{-31}\,\mathrm{kg}$$

Its corresponding rest energy is

$$W_e = m_e c^2 = 8.1871 \times 10^{-14}\,\mathrm{J} \approx 0.511\,\mathrm{MeV}$$

In the torus model, this energy is associated with the complete internal field configuration. The electric field E, magnetic field B, and motion-related field P participate in a periodic redistribution of energy.

The central energy requirement is therefore

$$W_{\mathrm{torus}} = m_e c^2$$

A consistent model must account for the contributions of all three fields without double-counting energy transferred between them.

2.2 Characteristic Frequency and Period

The electron rest energy defines a characteristic angular frequency through the energy–frequency relation

$$\omega_e = \frac{m_e c^2}{\hbar}$$

Numerically,

$$\omega_e \approx 7.7634 \times 10^{20}\ \mathrm{rad/s}$$

The corresponding characteristic period is

$$T_e = \frac{2\pi}{\omega_e} = \frac{h}{m_e c^2} \approx 8.09 \times 10^{-21}\ \mathrm{s}$$

This period provides a reference scale for the internal dynamics of the torus.

The electromagnetic torus is assumed to possess a fundamental closed mode with one complete phase cycle around its major circumference:

n = 1

The geometric phase-closure condition is

kR = 1

If the collective propagation velocity is denoted by v, the corresponding circulation period is

$$T_R = \frac{2\pi R}{v}$$

In the coupled E–B–P model, v is determined by the collective dynamics and need not equal c. Agreement between the resulting circulation period and the characteristic electron period provides one of the quantitative consistency tests.

The reference period derived from the electron rest energy is not itself an independent measurement of an internal electron oscillation.

2.3 Electric Charge

The experimentally observed electron charge is

$$Q_e = -e = -1.602176634 \times 10^{-19}\ \mathrm{C}$$

In the proposed structural model, the external electric field is investigated as a consequence of the spatial organization and periodic dynamics of the torus.

The internal electric field is assumed to undergo an asymmetric cycle. Electric-field components directed toward the center of the toroidal cross-section encounter opposing field contributions and the response of P. Outward-directed components may contribute to the surrounding electric field in the form of short, phase-distributed impulses.

The model therefore investigates whether the superposition of these contributions can produce the persistent external field associated with the electron.

At distances much larger than the torus dimensions, the required electric field is

$$E(r) \approx -\frac{e}{4\pi\varepsilon_0 r^2}\hat{r}$$

The corresponding total electric flux must satisfy

$$\oint_S E \cdot dA = -\frac{e}{\varepsilon_0}$$

These relations provide quantitative constraints on the proposed field structure. In particular, the model must establish how a nonzero net flux arises from the coupled E–B–P dynamics.

2.4 Intrinsic Angular Momentum

The electron possesses intrinsic angular momentum characterized by the spin quantum number

$$s = \frac{1}{2}$$

Its measured spin projection along a selected quantization axis has magnitude

$$|J_z| = \frac{\hbar}{2}$$

The corresponding spin magnitude in quantum mechanics is

$$|S| = \sqrt{s(s+1)}\hbar = \frac{\sqrt{3}}{2}$$

In the electromagnetic torus model, the axial angular momentum is investigated through the circulating field momentum.

The electric and magnetic field configurations are assumed to provide the persistent mean axial contribution. The P field participates in internal energy and momentum transfer, while its changing direction may result in a vanishing mean axial contribution:

$$\langle J_P \rangle = 0$$

The resulting mean angular-momentum condition is

$$\langle J_z \rangle = \langle J_E \rangle + \langle J_B \rangle$$

For comparison with the electron spin projection, the model must reproduce

$$|\langle J_z \rangle| \approx \frac{\hbar}{2}$$

This provides a quantitative target for the spatial distribution and circulation of electromagnetic energy. Reproducing this axial value does not by itself establish the full quantum behavior of spin one-half.

2.5 Magnetic Moment

The electron magnetic moment is closely related to its intrinsic angular momentum.

The Bohr magneton is

$$\mu_B = \frac{e\hbar}{2m_e} \approx 9.27401 \times 10^{-24}\,\mathrm{J/T}$$

The measured magnitude of the electron spin magnetic moment is approximately

$$|\mu_e| = 1.00115965\,\mu_B$$

In the torus model, the magnetic moment is associated with the effective circulation of the electric charge distribution.

For a phase-locked charge distribution rotating with angular frequency ω, the axial magnetic moment can be written as

$$\mu_z = \frac{\omega}{2}\int_V \rho_q(r)\; r_\perp^2\, dV$$

Here, the distance r_p is measured from the axis of circulation and the signed charge density determines the direction of the magnetic moment.

The magnetic moment is therefore sensitive not only to the total effective charge but also to its radial distribution.

An important question is whether the same toroidal geometry and field dynamics can account simultaneously for the electron angular momentum and magnetic moment.

Their measured relationship is characterized by the electron g-factor, whose magnitude is approximately

$$g_e \approx 2.00231930$$

The torus model must ultimately explain why the magnetic moment and angular momentum have this particular relationship.

2.6 Structural Stability

The electron is experimentally stable. A torus intended to represent the electron must therefore maintain its essential configuration despite continuous internal energy exchange and external interactions.

The proposed structure must satisfy several stability conditions.

First, the total internal energy must remain conserved in the stationary state, apart from explicitly modeled interactions with the environment.

Second, the coupled fields must sustain a coherent oscillation without progressively destroying their spatial organization.

Third, the saturated torus must possess a restoring mechanism that opposes small departures from its equilibrium geometry.

Finally, the stationary configuration must not continuously lose its rest energy through outward electromagnetic radiation.

The coupled motion of E, B, and P is investigated as a possible mechanism for

maintaining this balance. The energy-saturated state is expected to impose restrictions on the major radius R, minor radius a, and allowed internal modes.

2.7 Unified Constraints on the Electron Torus

The electron model must satisfy the principal measured constraints within one and the same structural configuration.

Property	Experimental reference	Torus-model requirement
Rest energy	0.511 MeV	Total internal energy
Characteristic period	8.09 zs from h/W	Compatible internal dynamics
Electric charge	−e	Correct external electric flux
Axial spin projection	ħ/2	Persistent axial angular momentum
Magnetic moment	1.00115965 μB	Appropriate effective current distribution
Gyromagnetic factor	2.00231930	Consistent relation between μ and J
Stability	Stable electron	Coherent, non-radiating saturated state

Table 1. *Experimental electron properties and corresponding requirements of the electromagnetic torus model. The table summarizes the principal physical constraints that a proposed electron structure must satisfy, including rest energy, electric charge, angular momentum, magnetic moment, and long-term stability. These requirements must be fulfilled within a single coherent electromagnetic configuration.*

The central objective is to determine whether these quantities can be connected through a limited number of geometrical and dynamical parameters rather than introduced as independent characteristics.

The following sections develop the geometry, internal energy exchange, and inertial behavior of the electromagnetic torus before comparing the resulting quantities with the measured properties of the electron. [1], [4]

3. Geometry of the Saturated Electromagnetic Torus

3.1 Basic Toroidal Geometry

The proposed electron structure is a closed electromagnetic torus characterized by two principal dimensions: the major radius R and the minor radius a.

The major radius R defines the distance between the central axis of the torus and the center of its cross-section. The minor radius a describes the characteristic transverse extent of the internal electromagnetic structure.

For an ideal torus with a circular cross-section, the volume is

$$V = 2\pi^2 R a^2$$

The inner and outer radial boundaries are

$$r_{\text{in}} = R - a$$

$$r_{\text{out}} = R + a$$

These boundaries are important because electromagnetic energy, momentum, and effective electric-current distributions need not be uniform across the cross-section.

In particular, the inner and outer regions follow different paths around the central axis. Consequently, even when the complete structure remains phase synchronized, their local field amplitudes, energy densities, and contributions to angular momentum and magnetic moment may differ.

The torus is therefore treated as a three-dimensional electromagnetic structure rather than a thin circular current loop.

3.2 Fundamental Closed Mode

A stable toroidal configuration requires both geometrical and phase closure.

The electromagnetic structure must return to its initial spatial position and internal phase after completing a circuit around the major circumference.

Let s denote the coordinate along this circumference and let the collective phase be

$$\phi(s,t) = ks - \omega t$$

For a closed mode, the total phase change around the circumference must be an integer multiple of 2π:

$$k(2\pi R) = 2\pi n$$

Therefore,

$$k = \frac{n}{R}$$

The present analysis concentrates on the fundamental mode

$$n = 1$$

for which

$$k = \frac{1}{R}$$

and

$$\lambda_\phi = 2\pi R$$

Thus, one complete phase cycle is distributed around the major circumference.

Higher-order modes are geometrically possible, but the fundamental mode is considered the principal candidate for the stable electron configuration.

The selection of n = 1 is treated as a structural hypothesis. Its stability relative to higher-order modes must ultimately follow from the coupled field dynamics and the conditions of energy saturation.

3.3 Helical Structure and Internal Circulation

The torus combines two forms of motion.

The first is the progression of the collective electromagnetic pattern around the major circumference R.

The second is the internal circulation and redistribution of field energy within the transverse cross-section.

These motions are coupled but need not possess identical characteristic velocities.

The resulting field structure may be represented geometrically as a helical organization in which the internal phase evolves while the collective pattern progresses around the torus.

For the simplest closed configuration, one internal circulation may correspond to one complete progression around the major circumference.

This geometrical relationship provides a possible foundation for the coupling between longitudinal propagation and transverse field oscillation.

However, geometrical closure alone does not determine the oscillation frequency. The frequency must also satisfy the dynamical conditions imposed by E, B, and P.

3.4 Different Local Velocities within the Cross-Section

The collective electromagnetic structure is assumed to possess a common angular phase velocity around the central axis.

Denoting this angular frequency by ω, the local tangential phase velocity at radial position r is

$$v_\phi(r) = \omega r$$

At the major radius,

$$v_R = \omega R$$

The corresponding inner and outer phase velocities are

$$v_{\text{in}} = \omega(R - a)$$

$$v_{\text{out}} = \omega(R + a)$$

Therefore,

$$\frac{v_{\text{out}}}{v_{\text{in}}} = \frac{R + a}{R - a}$$

The difference follows directly from the geometry of synchronous phase progression.

In the coupled E–B–P model, the characteristic velocity v_R is not required to equal c. The inertial response of P can reduce the collective phase-progression velocity while maintaining phase coherence between different regions of the torus.

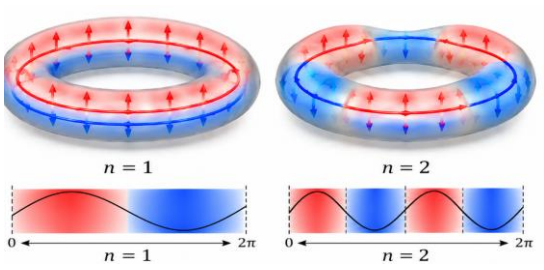


Figure 2. Comparison of closed toroidal modes with different phase numbers n. The present model identifies the electron with the fundamental saturated mode n=1.

The local velocities defined above describe the progression of the coherent field pattern. They must not automatically be identified with the transport velocities of energy, electric charge, or information.

This distinction is particularly important near the outer boundary, where the phase velocity may be greater than c without implying superluminal physical transport.

3.5 Spatial Organization of E, B, and P

The torus contains three mutually coupled field components with different dynamical roles.

The electric field E participates in the transverse redistribution of energy and produces electric stresses associated with the geometry of the structure.

The magnetic field B participates in the complementary part of the electromagnetic oscillation and contributes to the circulation and confinement of field energy.

The P field is assigned an independent inertial response. It mediates the transfer of energy between E and B and influences the collective motion of the complete structure.

The fields are not assumed to occupy identical spatial distributions.

Their characteristic amplitudes may be concentrated in different regions of the toroidal cross-section, and their local directions may change during the oscillation cycle.

The proposed energy-transfer sequence is

E → P → B → P → E.

This sequence permits the electric and magnetic energy maxima to occur at different stages of the cycle while P participates in both transitions.

Spatial coherence requires the three fields to remain dynamically coupled, but it does not require their instantaneous maxima to occur at the same position or time.

This distinction is essential for the later analysis of inertia, angular momentum, and the external electric field.

3.6 Circular and Elliptical Cross-Sections

A circular cross-section provides the simplest geometrical approximation. However, energy saturation and the different spatial distributions of E, B, and P may produce

unequal stresses in the radial and transverse directions.

Consequently, the equilibrium cross-section need not remain circular.

To describe a possible elliptical configuration, introduce two transverse semi-axes:

- a_r in the radial direction;
- a_z in the direction parallel to the central axis of the torus.

The corresponding volume is

$$V = 2\pi^2 R a_r a_z$$

The degree of cross-sectional deformation may be characterized by

$$\epsilon = \frac{a_z}{a_r}$$

For a circular cross-section,

$$\epsilon = 1$$

while deviations from unity describe elliptical deformation.

The purpose of introducing this possibility is not to add an independently adjustable geometrical parameter. Rather, the cross-sectional shape should ultimately follow from the spatial distribution of field stresses and the condition of mechanical and electromagnetic equilibrium.

The circular model will therefore remain the principal approximation until quantitative comparisons require a more detailed cross-sectional description.

3.7 Energy Saturation and Geometrical Constraints

The electron is assumed to correspond to an energy-saturated toroidal configuration.

During the formation and growth of electromagnetic toruses, changes in internal energy may be accompanied by changes in their characteristic dimensions and field distributions.

However, geometrical expansion cannot continue indefinitely while preserving the same internal organization.

As the torus approaches saturation, increasing field stresses and restrictions on transverse expansion may establish a preferred stable configuration.

The equilibrium geometry is expected to result from a balance between the tendencies associated with the electric, magnetic, and P fields.

The central condition can be expressed generally as the requirement that small geometrical perturbations produce restoring responses rather than unlimited expansion or contraction.

If the structural energy is represented by a function

$$W = W(R, a_r, a_z)$$

a stationary candidate configuration satisfies

$$\frac{\partial W}{\partial R} = 0$$

$$\frac{\partial W}{\partial a_r} = 0$$

$$\frac{\partial W}{\partial a_z} = 0$$

These conditions apply to an appropriate constrained structural-energy functional, with conserved quantities held fixed. A stable equilibrium additionally requires positive restoring stiffness for the allowed perturbations.

The present article does not attempt to reconstruct every stage of torus formation. Instead, it examines whether the resulting saturated geometry can support the physical properties of the electron.

3.8 Geometrical Scale of the Electron Torus

The electron rest energy provides a characteristic frequency scale through

$$\omega_e = \frac{m_e c^2}{\hbar}$$

The corresponding characteristic period is

$$T_e = \frac{2\pi}{\omega_e}$$

If the collective circulation period of the torus is identified with this reference period, the major radius must satisfy

$$2\pi R = v_R T_e$$

Therefore,

$$R = \frac{v_R}{c}\frac{\hbar}{m_e c}$$

Unlike the earlier model, which used $v_R = c$, the present model permits the collective propagation velocity to be reduced by the coupling with P.

In the strong-coupling approximation developed later, three comparable inertial contributions give

$$v_R \approx \sqrt{\frac{2}{3}}c$$

Substitution gives the indicative major radius

$$R \approx 3.15 \times 10^{-13}\ \mathrm{m}$$

or approximately 0.315 pm.

This value is a conditional geometric estimate obtained by identifying the circulation period with the characteristic period derived from the measured electron rest energy. It is not yet an independent prediction of the electron radius.

The minor radius and the detailed cross-sectional geometry remain to be constrained by the field-stability conditions and the simultaneous requirements of angular momentum and magnetic moment.

The resulting geometry will provide the basis for the quantitative calculations in the following sections.

3.9 Geometrical Framework for the Electron Model

The proposed electron torus is characterized by the following structural features:

1. A closed three-dimensional electromagnetic configuration with a major radius R and a finite transverse cross-section.
2. A fundamental phase-closed mode with n = 1.
3. A coupled helical organization of longitudinal progression and transverse internal motion.
4. Three interacting field components E, B, and P with potentially different spatial distributions.
5. A collective propagation velocity determined by field dynamics rather than imposed to equal c.
6. An energy-saturated configuration whose equilibrium dimensions are constrained by internal restoring forces.

These properties establish the geometrical framework required for the subsequent analysis.

The next section examines how the periodic transfer of energy between E, P, and B can occur while the complete structure maintains its coherence and characteristic geometry. [5], [7]

4. Energy Exchange Between E, P, and B

4.1 Three Coupled Fields

The electromagnetic torus is assumed to contain three dynamically coupled field components: the electric field E, the magnetic field B, and the motion-related field P.

Unlike a freely propagating electromagnetic wave, the internal configuration of the saturated torus is characterized by a periodic

redistribution of energy between these three components.

The electric and magnetic fields do not reach their energy maxima simultaneously. Instead, their maxima are separated by an intermediate state in which energy is predominantly associated with P.

The proposed sequence is

E → P → B → P → E.

In this description, P is not merely a passive medium connecting the electric and magnetic fields. It possesses an independent inertial response and temporarily stores energy during the transition between the electromagnetic configurations.

The three components therefore form one dynamically connected oscillating structure.

4.2 Idealized Energy-Exchange Cycle

To describe the sequence quantitatively, introduce a common phase variable

$$\theta = \Omega t$$

where Ω denotes the angular frequency of the internal energy-exchange cycle.

As a first approximation, let the energy contributions be represented by non-negative functions of θ.

The electric contribution is

$$W_E(\theta) = W_0 \cos^4\left(\frac{\theta}{2}\right)$$

The magnetic contribution is

$$W_B(\theta) = W_0 \sin^4\left(\frac{\theta}{2}\right)$$

The contribution of P is

$$W_P(\theta) = \frac{W_0}{2}\sin^2\theta$$

These expressions satisfy

$$W_E(\theta) + W_P(\theta) + W_B(\theta) = W_0$$

for every phase θ.

The total energy therefore remains constant throughout the complete cycle.

The characteristic states are:

Phase	Electric energy	P energy	Magnetic energy
θ = 0	Maximum	Zero	Zero
θ = π/2	Reduced	Maximum	Reduced
θ = π	Zero	Zero	Maximum
θ = 3π/2	Reduced	Maximum	Reduced
θ = 2π	Maximum	Zero	Zero

Table 2. *Energy redistribution during one complete E–P–B oscillation cycle. The table identifies the characteristic stages of the periodic transfer E → P → B → P → E. The three energy contributions vary continuously, while their total remains constant. The intermediate P-field maxima represent the transition between electric- and magnetic-dominated states.*

The energy transfer is continuous. The notation E → P → B → P → E expresses the dominant direction of energy redistribution, not an instantaneous disappearance of one field followed by the appearance of another.

In particular, the intermediate states need not contain energy exclusively in P. All three components may coexist while their relative contributions change.

This distinction is important because coherent coupling requires continuous interaction between the fields.

The non-negative energy contributions introduced here describe an idealized redistribution of the conserved total energy. They should be distinguished from the signed structural energy balance developed in Part A1,

where the magnetic binding contribution is assigned a negative sign. The relationship between these two descriptions requires a consistent energy accounting in the complete field model.

4.3 Energy Conservation and Transfer Rates

The internal energy balance is

$$W_E + W_B + W_P = W_0$$

Consequently,

$$\frac{dW_E}{dt} + \frac{dW_B}{dt} + \frac{dW_P}{dt} = 0$$

The energy-transfer rates can be expressed as

$$\frac{dW_E}{dt} = -2\Omega W_0 \cos^3\left(\frac{\theta}{2}\right)\sin\left(\frac{\theta}{2}\right)$$

$$\frac{dW_B}{dt} = 2\Omega W_0 \sin^3\left(\frac{\theta}{2}\right)\cos\left(\frac{\theta}{2}\right)$$

$$\frac{dW_P}{dt} = 2\Omega W_0 \sin\theta\cos\theta$$

Their sum is identically zero.

During the first half of the cycle, electric energy decreases while magnetic energy increases. The P contribution first increases and subsequently decreases, thereby representing an intermediate stage in the transfer process.

During the second half, the process reverses: magnetic energy decreases, P again participates in the transition, and electric energy returns to its maximum.

The signs of the derivatives identify the instantaneous directions of energy redistribution. The P field alternately receives and releases energy while the total energy remains constant.

The complete cycle therefore conserves energy without requiring E and B to oscillate in phase.

4.4 The Inertial Role of P

The field P account for an inertial component of the internal electromagnetic motion.

In the proposed model, energy transfer between E and B is not instantaneous. The P field responds to the changing electromagnetic configuration and may temporarily retain energy associated with that response.

Its behavior is therefore characterized by two related properties: the capacity to store energy and resistance to changes in its motion.

In a simplified dynamical description, introduce an effective coordinate p associated with the P field. Its inertial response may be represented by

$$M_P\ddot{p} = F_{EB\to P}$$

where M_P is an effective inertial coefficient and F represents the combined action of the electric and magnetic field configuration on P.

The reaction of P acts back on E and B, establishing a coupled system rather than a one-directional transfer mechanism.

The effective inertial coefficients of E, B, and P are assumed to be comparable when the corresponding field contributions reach their characteristic maxima.

This is a working approximation intended to investigate collective motion. It does not imply that the instantaneous energies of all three fields are equal.

4.5 Phase Relations Between the Fields

In a freely propagating electromagnetic wave, E and B can vary coherently and in phase at a fixed position.

The proposed electron torus is based on a different internal oscillation.

Electric and magnetic energy reach their maxima at different phases, with the P field participating in the intermediate stages.

The resulting energy sequence has a full period of 2π in θ:

$$W_i(\theta + 2\pi) = W_i(\theta)$$

The field amplitudes themselves may have a longer signed period than their corresponding energy densities.

This distinction matters because energy depends quadratically on field amplitude, whereas the direction of a field is determined by its sign and spatial orientation.

The present energy model specifies the redistribution of non-negative energy contributions. A complete dynamical field solution must additionally determine the vector directions and phase relationships of E, B, and P.

4.6 Local Exchange and Collective Circulation

Two characteristic motions must be distinguished.

The first is the local exchange of energy between E, P, and B within the toroidal cross-section.

The second is the collective progression of the connected electromagnetic pattern around the major circumference R.

The local exchange frequency Ω is associated with the internal redistribution of energy.

The collective angular frequency ω is related to progression around the major circumference:

$$\omega = \frac{v_R}{R}$$

These frequencies need not be identical by definition.

For a stable phase-locked configuration, however, their relationship must satisfy a resonance or periodic-closure condition.

In the simplest case, one complete internal energy-exchange cycle occurs during one revolution of the collective pattern:

$$\Omega = \omega$$

More general configurations may permit integer frequency ratios, but the present article concentrates on the simplest closed mode.

The resonance condition connects transverse internal dynamics with longitudinal phase progression and is expected to contribute to the selection of stable toroidal configurations.

4.7 Energy Exchange and Angular Momentum

The periodic transfer of energy does not require all three fields to contribute equally to the mean axial angular momentum.

In the present model, the electric and magnetic configurations are assumed to provide the persistent mean axial contribution.

The P field changes its local direction during the oscillation cycle. Its signed axial angular-momentum contribution may therefore have zero time average:

$$\langle J_P \rangle = 0$$

The mean axial angular momentum is then

$$\langle J_z \rangle = \langle J_E \rangle + \langle J_B \rangle$$

Nevertheless, P can participate in the instantaneous redistribution of momentum during the energy-transfer cycle.

The complete torus must conserve its total angular momentum in the absence of external torque and radiation.

Thus, zero mean angular momentum of P does not imply an absence of inertial or dynamical influence.

The detailed spatial distribution of angular momentum will be examined in Section 7.

4.8 Energy Exchange in the Saturated State

The saturated torus is assumed to maintain a stable periodic configuration despite continuous internal motion.

The energy-transfer cycle does not represent repeated creation and destruction of electromagnetic energy. Instead, the same total internal energy is redistributed between the coupled field components.

A stable cycle requires that changes in field amplitudes, geometry, and inertial response remain mutually compatible.

The internal redistribution of energy may generate temporary stresses and local momentum transfer, but these processes must not lead to cumulative deformation or continuous outward radiation in the stationary state.

The presence of P provides a possible inertial mechanism for maintaining phase coherence and moderating the collective response of the torus.

The idealized energy functions developed above demonstrate that the required transfer sequence is compatible with conservation of total energy.

They do not yet establish the detailed forces that generate the cycle. Those forces must ultimately be derived from the coupled dynamics of E, B, and P.

4.9 Summary

The proposed electron torus contains a periodic internal energy-exchange mechanism characterized by the sequence

E → P → B → P → E.

A continuous mathematical representation has been constructed in which the three energy contributions remain non-negative and their sum is constant throughout the cycle.

The P field participates in both transitions between electric and magnetic energy and is assigned an independent inertial response.

The internal energy-exchange cycle is distinguished from the collective progression of the torus around its major circumference. Their coupling provides the basis for investigating the characteristic frequency and propagation velocity of the saturated structure.

The next section develops a simplified dynamical model of the three inertial field components and examines how their coupling can reduce the collective propagation velocity below c. [2], [7]

5. Field Inertia and Collective Motion

5.1 Inertia of the Three Field Components

The electromagnetic torus is assumed to contain three dynamically coupled fields: E, B, and P. Each field possesses its own inertial response and participates in the collective motion of the complete structure.

Inertia is understood here as the resistance of a field configuration to changes in its state of motion. The electric and magnetic components contribute to the propagation and redistribution of electromagnetic energy, while P provides an additional inertial degree of freedom.

An essential assumption of the model is that the characteristic inertial coefficients of E, B, and P are comparable. In the simplest approximation, they are taken to be equal:

$$M_E = M_B = M_P = M_0$$

This equality refers to their characteristic dynamical coefficients, not to their instantaneous stored energies.

During the energy-exchange cycle developed in Section 4, the energy contributions of E, B, and P vary continuously. Nevertheless, all three fields remain dynamically connected and contribute to the collective response of the torus.

The objective of this section is to determine how their coupling affects the velocity of the common electromagnetic pattern.

5.2 Collective Propagation and Internal Motion

Two forms of motion must be distinguished.

The first is the local redistribution of energy between E, P, and B. This process involves changes in field amplitudes, directions, and local momentum.

The second is the progression of the connected field configuration around the major circumference of the torus.

The collective phase is represented by

$$\phi(s,t) = ks - \omega t$$

For the fundamental closed mode,

$$n = 1, \qquad k = \frac{1}{R}$$

The corresponding phase-progression velocity is

$$v_R = \frac{\omega}{k} = \omega R$$

In a freely propagating electromagnetic mode, the characteristic propagation velocity is c. In the proposed torus, however, the electromagnetic components remain coupled to P.

The collective velocity is therefore determined by the response of the entire coupled structure rather than by the uncoupled electromagnetic components alone.

The inertia of P can reduce the common phase-progression velocity without requiring the local electromagnetic interactions to operate independently at that reduced velocity.

5.3 A Simplified Three-Field Dynamical Model

To investigate this effect, introduce three effective displacement coordinates along the major circumference:

$$q_E(s,t), \qquad q_B(s,t), \qquad q_P(s,t)$$

These coordinates represent dynamical perturbations of the three coupled field configurations. They are not the electric and magnetic field strengths themselves.

The E and B coordinates are assigned equal longitudinal propagation stiffness, corresponding to the characteristic velocity c in the uncoupled approximation.

The P coordinate possesses inertia but is initially assumed to have negligible independent longitudinal propagation stiffness.

The interaction between the three coordinates is represented by a common coupling coefficient K.

With equal inertial coefficients M_0, the equations of motion become

$$\ddot{q_E} = c^2 \frac{\partial^2 q_E}{\partial s^2} - \gamma(2q_E - q_B - q_P)$$

$$\ddot{q_B} = c^2 \frac{\partial^2 q_B}{\partial s^2} - \gamma(2q_B - q_E - q_P)$$

$$\ddot{q_P} = -\gamma(2q_P - q_E - q_B)$$

where

$$\gamma = \frac{K}{M_0}$$

The coupling terms describe restoring interactions between the relative configurations of the three fields.

Each field is represented by an independent dynamical coordinate, and the interaction forces act reciprocally.

The model is deliberately minimal. It is intended to determine the consequences of three coupled inertial components, not to replace the full electromagnetic field equations.

5.4 Conservation of the Dynamical Energy

The coupled equations admit a conserved positive quadratic energy in the absence of external interactions.

The corresponding total energy is

$$W_{\mathrm{dyn}} = \frac{M_0}{2}\int_0^{2\pi R}\Big[\dot{q}_E^2 + \dot{q}_B^2 + \dot{q}_P^2 + c^2\left(\frac{\partial q_E}{\partial s}\right)^2 + c^2\left(\frac{\partial q_B}{\partial s}\right)^2 + \gamma((q_E - q_B)^2 + (q_B - q_P)^2 + (q_P - q_E)^2)\Big]ds$$

The kinetic terms describe the inertial response of the three components, while the gradient and coupling terms describe the restoring interactions.

For periodic boundary conditions around the torus, differentiation of this expression using the equations of motion gives

$$\frac{dW_{\mathrm{dyn}}}{dt} = 0$$

Thus, the simplified model permits energy exchange between the three dynamical components without requiring a net change in total energy.

The conserved quantity W_{dyn} describes the perturbation dynamics. Its separate contributions must not be identified directly with the field-energy functions W_E, W_B, and W_P introduced in Section 4 without an additional constitutive relation.

5.5 Fundamental Mode and Characteristic Frequencies

For the fundamental closed mode, the three coordinates may be represented as

$$q_i(s,t) = A_i e^{i(s/R - \omega t)}$$

Introduce the dimensionless quantities

$$g = \frac{\gamma R^2}{c^2}, \qquad x = \frac{\omega^2 R^2}{c^2}$$

Substitution into the coupled equations leads to the following characteristic matrix:

$$\begin{pmatrix} 1+2g-x & -g & -g \\ -g & 1+2g-x & -g \\ -g & -g & 2g-x \end{pmatrix}\begin{pmatrix} A_E \\ A_B A_P \end{pmatrix} = 0$$

The system has three characteristic modes.

Two modes involve the symmetric combination of E and B with P. Their dimensionless eigenvalues are

$$x_{\pm} = \frac{1 + 3g \pm \sqrt{1 - 2g + 9g^2}}{2}$$

The third mode is associated with opposite dynamical displacements of E and B while P remains unexcited:

$$x_A = 1 + 3g$$

The lower-frequency mode, x_A, describes the slow collective response of the coupled structure.

The higher-frequency modes describe relative motion between the field coordinates.

In general, a perturbation can excite more than one mode. A coherent stationary configuration therefore requires a suitable selection or phase locking of its internal oscillations.

5.6 Collective Velocity in the Strong-Coupling Limit

The most important result follows when the coupling is sufficiently strong that the relative displacements of E, B, and P remain small.

The three coordinates then move approximately together:

$$q_E \approx q_B \approx q_P$$

In this limit, the three inertial contributions participate in the common motion.

The E and B components provide two equal contributions to the longitudinal propagation stiffness, while P contributes an additional inertial response.

The resulting effective velocity satisfies

$$v_R^2 = \frac{M_E c^2 + M_B c^2}{M_E + M_B + M_P}$$

For equal inertial coefficients,

$$M_E = M_B = M_P = M_0$$

this becomes

$$v_R^2 = \frac{2M_0c^2}{3M_0}$$

and therefore

$$v_R = \sqrt{\frac{2}{3}}c$$

Numerically,

$$v_R \approx 0.8165c$$

The collective phase progression is therefore approximately 18.4% slower than c.

This reduction is not introduced as an independent velocity parameter. It follows from the assumed equality of the three inertial coefficients and the assignment of longitudinal restoring stiffness to E and B.

The result is a limiting value of the simplified coupled model. For finite coupling, the collective velocity is somewhat lower.

5.7 Dependence on the Coupling Strength

For finite coupling, the slow-mode velocity is obtained from the lower eigenvalue:

$$v_-(g) = c\sqrt{\frac{1 + 3g - \sqrt{1 - 2g + 9g^2}}{2}}$$

Several representative values are shown below.

Coupling g	Collective phase velocity
0.25	0.600c
1	0.765c
4	0.805c
20	0.814c
Strong-coupling limit	0.8165c

***Table 3**. Dependence of the collective phase velocity on the field-coupling strength. Increasing the coupling parameter (g) progressively synchronizes the three inertial field components and raises the velocity of the slow collective mode toward its limiting value of approximately (0.8165c). The limit follows from the assumed equal inertial coefficients of E, B, and P and the propagation stiffness assigned to E and B.*

The model therefore predicts a continuous increase in the collective phase velocity as the coupling becomes stronger, approaching a limiting value below c.

In this approximation, the inertia of P remains dynamically important even when the coupling becomes very strong.

The coupling parameter itself has not yet been determined from the microscopic field structure. Its value must ultimately be connected with the electromagnetic stresses and the inertial properties of P.

5.8 Relationship to the Energy-Exchange Cycle

The collective propagation model and the energy-exchange model describe complementary aspects of the torus.

Section 4 introduced the periodic sequence

E → P → B → P → E

and demonstrated that non-negative energy contributions can be redistributed while their sum remains constant.

The present section shows that three independent but coupled inertial coordinates can support a slower common mode.

These results are compatible in principle, but they do not yet constitute a complete dynamical derivation of the same physical oscillation.

In particular, the symmetric collective mode represents approximately equal dynamical displacements of the E and B coordinates. This should not be interpreted as requiring the physical electric and magnetic field energies to reach their maxima simultaneously.

A full description must relate the effective dynamical coordinates to the physical field amplitudes and their phase-shifted energy exchange.

The P field is therefore assigned two connected roles: it participates in the internal energy-transfer cycle and modifies the inertial response of the common toroidal mode.

5.9 Consequences for the Electron Torus

The collective velocity determines the circulation period around the major circumference:

$$T_R = \frac{2\pi R}{v_R}$$

Using the strong-coupling result,

$$T_R = \sqrt{\frac{3}{2}}\frac{2\pi R}{c}$$

Thus, a torus with a given major radius possesses a longer collective circulation period than the corresponding uncoupled electromagnetic configuration.

Conversely, if the collective period is constrained by the characteristic period associated with the electron rest energy, the required major radius is reduced.

The quantitative connection between the circulation period, electron rest energy, and toroidal dimensions is developed in Section 6.

The principal result of the present section is that the participation of P provides a specific inertial mechanism for slowing the collective electromagnetic pattern.

This mechanism preserves the independent dynamical roles of E, B, and P while connecting them through a single coherent mode.

5.10 Summary

A simplified three-field dynamical model has been developed to investigate the collective motion of the electromagnetic torus.

The model assigns equal characteristic inertial coefficients to E, B, and P, with reciprocal coupling between all three components.

Its fundamental closed mode contains a slow collective response and faster internal modes. In the strong-coupling limit, the collective phase velocity approaches

$$v_R = \sqrt{\frac{2}{3}}c \approx 0.8165c$$

The reduction follows from the additional inertial contribution of P and does not require an independent adjustment of the propagation velocity.

The model also possesses a conserved dynamical energy, demonstrating that coupled internal motion need not produce net energy loss.

The result establishes a quantitative link between field inertia and the characteristic circulation of the torus.

The following section examines whether the resulting circulation period and geometric scale are compatible with the measured rest energy of the electron. [2], [3]

6. Electron Energy and Characteristic Period

6.1 Electron Rest Energy as a Quantitative Constraint

The electron possesses a precisely measured rest energy. Any electromagnetic torus proposed as its internal structure must reproduce this energy while maintaining a stable, coherent field configuration.

The measured electron rest energy is

$$W_e = m_e c^2$$

Numerically,

$$W_e = 8.1871 \times 10^{-14}\,\mathrm{J} = 0.510999\,\mathrm{MeV}$$

In the proposed model, this energy is associated with the complete coupled configuration of E, B, and P.

During the periodic cycle described in Section 4, the energy is redistributed between the three components:

$$W_E(t) + W_P(t) + W_B(t) = W_e$$

The total remains constant, although the individual contributions vary.

This distinction is fundamental. The mass-energy of the electron is attributed to the complete electromagnetic structure, rather than to a single field component or to the instantaneous energy maximum of one field.

The equality between the total torus energy and the measured electron rest energy is introduced as a physical constraint. The purpose of the following calculation is to determine the geometrical dimensions and characteristic motion compatible with that constraint.

6.2 Characteristic Frequency Associated with Electron Energy

The relation between energy and angular frequency provides a characteristic frequency scale:

$$W_e = \hbar\omega_e$$

Therefore,

$$\omega_e = \frac{m_e c^2}{\hbar}$$

Substitution gives

$$\omega_e = 7.7634 \times 10^{20}\ \mathrm{rad/s}$$

The corresponding ordinary frequency is

$$f_e = \frac{\omega_e}{2\pi} = 1.2356 \times 10^{20}\ \mathrm{Hz}$$

and the characteristic period is

$$T_e = \frac{1}{f_e} = \frac{h}{m_e c^2}$$

Numerically,

$$T_e = 8.0933 \times 10^{-21}\ \mathrm{s}$$

This is the characteristic period associated with the electron rest energy, commonly called the Compton period.

It is not an independently measured period of internal electron motion. In the present model, it provides a reference for examining whether a closed electromagnetic torus can support a corresponding periodic configuration.

6.3 Circulation Period of the Fundamental Toroidal Mode

Section 3 established the phase-closure condition for the fundamental mode:

$$n = 1, \qquad k = \frac{1}{R}$$

The collective phase-progression velocity is

$$v_R = \frac{\omega}{k} = \omega R$$

The time required for one complete phase progression around the major circumference is consequently

$$T_R = \frac{2\pi R}{v_R}$$

In the preceding article, the simplest electromagnetic approximation associated the collective propagation velocity with c.

The present model introduces an additional inertial contribution from P. Consequently, the collective velocity need not equal c.

Section 5 showed that, in the strong-coupling limit with three equal inertial coefficients, the collective velocity approaches

$$v_R = \sqrt{\frac{2}{3}}c$$

or

$$v_R \approx 0.8165c$$

The corresponding circulation period becomes

$$T_R = \sqrt{\frac{3}{2}}\frac{2\pi R}{c}$$

Thus, for the same major radius, the coupled structure possesses a longer circulation period than an electromagnetic mode whose phase velocity equals c.

6.4 Major Radius Corresponding to the Electron Period

The simplest resonance hypothesis identifies one complete collective circulation with the characteristic period associated with the electron rest energy:

$$T_R = T_e$$

Combining the preceding relations gives

$$\frac{2\pi R}{v_R} = \frac{h}{m_e c^2}$$

Solving for the major radius,

$$R = \frac{v_R h}{2\pi m_e c^2}$$

or equivalently,

$$R = \frac{v_R}{c}\frac{\hbar}{m_e c}$$

The quantity

$$\overline{\lambda_C} = \frac{\hbar}{m_e c}$$

is the reduced Compton wavelength of the electron.

Therefore,

$$R = \frac{v_R}{c}\overline{\lambda_C}$$

For the strong-coupling velocity,

$$R = \sqrt{\frac{2}{3}}\overline{\lambda_C}$$

Numerically,

$$\overline{\lambda_C} = 3.86159 \times 10^{-13}\ \mathrm{m}$$

and hence

$$R = 3.15298 \times 10^{-13}\ \mathrm{m}$$

or approximately

$$R = 0.3153\ \mathrm{pm}$$

This is the characteristic major radius required for the fundamental collective mode to complete one circulation during the reference electron period.

The reduced radius follows from the participation of P in the common inertial response.

6.5 Dependence on the Field Coupling

The velocity derived in Section 5 represents the strong-coupling limit.

For finite coupling, the slow collective mode has the velocity

$$v_-(g) = c\sqrt{\frac{1 + 3g - \sqrt{1 - 2g + 9g^2}}{2}}$$

where g is the dimensionless coupling strength.

If the circulation period is constrained to equal the characteristic electron period, the major radius becomes

$$R(g) = \frac{v_-(g)}{c}\overline{\lambda_C}$$

Representative results are shown in Table 4.

Coupling g	Velocity v/c	Major radius R (pm)
0.25	0.600	0.2316
1	0.765	0.2956
4	0.805	0.3108
20	0.814	0.3144
Strong-coupling limit	0.8165	0.3153

Table 4. Collective propagation velocity and corresponding major radius for the fundamental mode.

The calculated radius approaches a limiting value as the coupling becomes stronger.

This behavior is relevant because the torus is assumed to represent a strongly coupled,

energy-saturated structure. In such a state, the three fields are expected to maintain a coherent collective motion despite the continuous redistribution of their internal energy.

The absolute coupling strength has not yet been derived from the electromagnetic field structure. Consequently, the strong-coupling limit provides a useful reference configuration, rather than a uniquely determined microscopic solution.

6.6 Transverse Geometry and Mean Energy Density

The preceding calculation determines a characteristic major radius but does not independently establish the minor radius or detailed cross-sectional shape.

For an initial estimate, consider a circular cross-section with the working geometrical ratio

$$\beta = \frac{a}{R} = 0.25$$

This value is adopted only as an illustrative geometry inherited from the earlier reduced torus model.

With

$$R = 0.3153\,\mathrm{pm}$$

the minor radius becomes

$$a = 0.0788\,\mathrm{pm}$$

The toroidal volume is

$$V = 2\pi^2 R a^2$$

which gives

$$V \approx 3.87 \times 10^{-38}\,\mathrm{m}^3$$

If the complete electron rest energy is assigned to this effective volume, the mean total energy density is

$$\bar{u} = \frac{W_e}{V}$$

Numerically,

$$\bar{u} \approx 2.12 \times 10^{24}\,\mathrm{J/m}^3$$

This value establishes the characteristic energy-density scale required by the proposed geometry.

It does not determine the individual electric, magnetic, or P-field amplitudes. Such a determination requires a specified relation between field amplitudes and their stored energies, including the contribution associated with P.

In particular, the P-field energy must not be added to an electromagnetic energy expression if it already represents energy accounted for elsewhere in the coupled system.

The purpose of the present estimate is therefore to establish the overall geometric and energetic scale, not to assume a detailed internal energy distribution.

6.7 Internal Energy Exchange and Collective Period

The torus supports two conceptually distinct processes.

The first is the redistribution of energy between E, P, and B:

E → P → B → P → E.

The second is the collective progression of the connected pattern around the major circumference.

The characteristic frequency of internal energy exchange is denoted by Ω, while the collective circulation frequency is ω.

For a coherent closed structure, the two motions must remain dynamically compatible.

The simplest hypothesis is a one-to-one resonance:

$$\Omega = \omega$$

Under this condition, one internal energy-exchange cycle corresponds to one complete

collective phase progression around the major circumference.

The energy-transfer functions introduced in Section 4 provide a periodic and energy-conserving representation of such a cycle.

However, the simplified inertial equations of Section 5 do not yet independently derive the complete E–P–B transfer sequence. The resonance condition therefore remains a structural requirement to be examined together with the detailed field dynamics.

Its significance is that a stable torus may possess a single characteristic frequency connecting its internal energy redistribution with its closed geometry.

6.8 Energy, Inertia, and Electron Mass

The connection between collective field inertia and electron rest energy is central to the proposed model.

The participation of P increases the inertial response of the coupled structure and reduces its collective propagation velocity.

The total stored energy, however, remains constrained by

$$W_e = m_e c^2$$

These two statements describe different aspects of the model.

The first concerns the dynamical response of coupled field configurations. The second concerns the energy associated with the complete electron.

The equality of the three characteristic inertial coefficients does not imply that the rest energy is divided into three equal constant portions.

Indeed, the idealized exchange cycle of Section 4 contains time-dependent energy contributions with different maxima and time averages.

A complete structural derivation of electron mass would require a field-energy functional and dynamical equations that establish the rest energy of the stable configuration without inserting the experimentally measured value.

The present calculation establishes a conditional relationship between measured electron energy, the collective circulation period, and the geometry of the torus.

6.9 Result of the Period and Energy Comparison

The simplified model leads to a direct geometrical consequence.

For the fundamental mode, three equal characteristic inertial coefficients and strong coupling give

$$v_R \approx 0.8165c$$

When the collective circulation period is identified with the characteristic electron period,

$$T_R = T_e = 8.0933 \times 10^{-21}\,\mathrm{s}$$

the major radius is

$$R \approx 0.3153\,\mathrm{pm}$$

This calculation connects three features within one framework: collective field inertia, phase-closed toroidal geometry, and the energy-derived characteristic period of the electron.

The result is not an independent prediction of electron mass, because the measured electron rest energy determines the reference period. Nevertheless, it provides a definite geometrical scale for subsequent consistency tests.

Most importantly, the resulting radius and velocity can now be used to examine whether the same torus can reproduce the electron angular momentum and magnetic moment.

The following sections investigate these properties without introducing a different toroidal geometry for each observable. [1], [3]

7. Angular Momentum and Spin

7.1 Angular Momentum as a Constraint on the Torus

The intrinsic angular momentum of the electron is one of the principal quantities that the proposed electromagnetic torus must reproduce.

The electron has spin quantum number s = 1/2. The magnitude of its spin projection along a selected quantization axis is

$$|S_z| = \frac{\hbar}{2}$$

The corresponding numerical value is

$$|S_z| = 5.27286 \times 10^{-35}\ \mathrm{J\,s}$$

In the proposed torus model, axial angular momentum is investigated as a consequence of the internal circulation of field momentum.

The electric and magnetic components contribute to the persistent mean angular momentum. The P field participates in the internal redistribution of energy and momentum but is assumed to reverse its axial contribution periodically, producing a zero time average.

The central quantitative question is whether the geometry and energy distribution established in the preceding sections can yield an axial angular momentum close to the electron reference value.

7.2 Angular Momentum of a Distributed Field Configuration

Electromagnetic fields carry momentum. In conventional electromagnetic theory, the momentum density is

$$g_{EM} = \frac{E \times B}{\mu_0 c^2}$$

The corresponding angular momentum about the torus axis is

$$J_z = \int_V [r \times g_{EM}]_z \, dV$$

In the proposed model, the P field introduces an additional dynamical contribution.

For a first quantitative estimate, the energy circulation may be represented by effective field contributions.

If an energy contribution W_i circulates at characteristic radius r_i with tangential velocity v_i, its effective axial angular momentum is approximated by

$$J_i = \sigma_i \frac{W_i v_i r_i}{c^2}$$

The factor σ_i describes the direction of its axial contribution.

For a phase-locked configuration with common angular velocity ω,

$$v_i = \omega r_i$$

and therefore

$$J_i = \sigma_i \frac{W_i \omega r_i^2}{c^2}$$

This relation provides a reduced geometrical estimate. The separate E and B contributions represent effective energy-flow components; they are not independently defined electromagnetic momentum densities. A complete calculation must recover their combined contribution from the field momentum and the dynamics of P.

7.3 Mean Angular Momentum of E, B, and P

The total angular momentum is written schematically as

$$J_z(t) = J_E(t) + J_B(t) + J_P(t)$$

The proposed P field changes the direction of its internal motion during the energy-exchange cycle.

Its mean axial contribution is assumed to vanish:

$$\langle J_P \rangle = 0$$

Consequently,

$$\langle J_z \rangle = \langle J_E \rangle + \langle J_B \rangle$$

This does not imply that P is dynamically inactive. It remains involved in the transfer of energy and may temporarily exchange momentum with the electromagnetic configuration.

The distinction between instantaneous and time-averaged angular momentum is important. The mean contributions of E and B determine the result of the reduced calculation, while the complete torus must also satisfy the conservation law for total angular momentum.

7.4 Energy Fractions from the Internal Exchange Cycle

Section 4 introduced the periodic energy redistribution

E → P → B → P → E.

For the idealized functions used there, the time-averaged energy fractions are

$$\langle W_E \rangle = \frac{3}{8} W_0$$

$$\langle W_B \rangle = \frac{3}{8} W_0$$

$$\langle W_P \rangle = \frac{1}{4} W_0$$

The complete energy is constrained by the electron rest energy:

$$W_0 = m_e c^2$$

An important consequence is that E and B have equal mean energy contributions, although their maxima occur at different phases.

These fractions were obtained from the energy-conserving exchange model and were not selected to reproduce electron angular momentum.

They therefore provide a useful input for an additional quantitative consistency test.

7.5 Geometrical Distribution of the Angular Momentum

The torus has a finite transverse cross-section. Its energy distribution is not restricted to the major radius R.

For the initial calculation, consider two characteristic effective circulation radii:

$$r_E = 0.75R$$

$$r_B = 1.25R$$

The selected radii represent effective positions of the circulating field-energy contributions rather than sharply localized field boundaries. The electric contribution is associated with the inner region of the toroidal cross-section, while the magnetic contribution is concentrated closer to its outer region. The actual effective radii must ultimately be determined from the corresponding spatial energy and momentum distributions.

These values represent an inner electric-dominated region and an outer magnetic-dominated region.

They are illustrative spatial positions, not geometrical results derived from the complete field equations.

The collective phase velocity from Section 5 is

$$v_R = \sqrt{\frac{2}{3}} c$$

and the common angular frequency is

$$\omega = \frac{v_R}{R}$$

The principal geometrical parameters from Section 6 are

$$R = 3.153 \times 10^{-13}\ \mathrm{m}$$

The local phase velocities at the selected radii are therefore

$$v_E = 0.75 v_R \approx 0.6124c$$

$$v_B = 1.20 v_R \approx 0.9798c$$

Both values remain below c.

These velocities describe the local progression of the phase-locked field pattern. Their use in the subsequent angular-momentum estimate assumes that the effective circulation of field energy can be represented by the same angular frequency. This relationship must ultimately follow from the complete field-momentum distribution.

For the present estimate, the mean axial contributions of E and B are taken to have the same orientation.

The physical justification of these effective directions remains part of the detailed field-structure problem.

7.6 Quantitative Calculation

Using the effective circulation approximation, the mean angular momentum becomes

$$\langle J_z \rangle = \frac{\omega}{c^2}(\langle W_E \rangle r_E^2 + \langle W_B \rangle r_B^2)$$

Substituting the energy fractions gives

$$\langle J_z \rangle = \frac{3W_0 \omega R^2}{8c^2}(0.75^2 + 1.20^2)$$

Since

$$W_0 = m_e c^2$$

and

$$R = \frac{v_R}{c}\frac{\hbar}{m_e c}$$

the angular momentum can be expressed in dimensionless form as

$$\frac{\langle J_z \rangle}{\hbar} = \frac{3}{8}\left(\frac{v_R}{c}\right)^2 (0.75^2 + 1.20^2)$$

Using

$$\left(\frac{v_R}{c}\right)^2 = \frac{2}{3}$$

gives

$$\frac{\langle J_z \rangle}{\hbar} = \frac{1}{4}(0.5625 + 1.4400)$$

Therefore,

$$\langle J_z \rangle = 0.500625$$

The electron reference value is

$$|S_z| = 0.500000$$

The relative difference is approximately 0.125%.

Thus, within the chosen effective field-distribution model, the calculated mean angular momentum lies very close to the electron spin projection.

This agreement follows from combining the energy fractions of Section 4, the collective velocity of Section 5, the major radius of Section 6, and the selected radial positions of the circulating field contributions.

The close agreement results from combining the energy fractions obtained in Section 4, the collective velocity derived in Section 5, the major radius established in Section 6, and the illustrative radial distribution introduced in Section 7.5. The calculation demonstrates that the required electron angular-momentum scale is compatible with the proposed toroidal geometry. The effective radial positions remain to be determined from the complete field-momentum distribution, and the resulting agreement should therefore be regarded as a quantitative consistency test rather than an independent prediction of electron spin.

7.7 Instantaneous Angular Momentum and Conservation

The periodic redistribution of energy between E, P, and B does not, by itself, imply a change in the total angular momentum of the torus. The three fields form a single coupled structure, and their internal energy exchange does not change its total energy.

In the proposed stationary configuration, the torus maintains its geometry, collective circulation, and total energy. Under these conditions, its total angular momentum is assumed to remain constant throughout the oscillation cycle.

The P field undergoes periodic acceleration and deceleration as energy is transferred between the field components. These internal processes must preserve the angular momentum of the complete structure.

For an isolated torus, the conservation condition is

$$\frac{dJ_{\text{total},z}}{dt} = 0$$

The present model adopts this conservation requirement without attempting a detailed calculation of the internal torques between E, B, and P.

7.8 Relationship Between Angular Momentum and Magnetic Moment

The angular momentum of the proposed torus depends on its internal momentum flow, whereas the magnetic moment depends on the effective electric-current distribution.

These distributions need not have identical radial dependence.

For a phase-locked circulation of effective charge density ρ_q, the magnetic moment may be represented by

$$\mu_z = \frac{\omega}{2}\int_V \rho_q(r) r_\perp^2 \, dV$$

The electron magnetic moment therefore provides a separate geometrical constraint on the same torus.

A satisfactory model must reproduce the angular momentum and magnetic moment simultaneously, without assigning a different major radius or collective frequency to each observable.

The relationship is especially restrictive because the measured electron gyromagnetic factor is close to two.

The present angular-momentum calculation provides one part of this comparison. The corresponding charge and current distributions are examined in the following sections.

7.9 Angular Momentum and Quantum Spin

The calculated quantity represents the mean axial angular momentum of an idealized circulating field configuration.

The quantum spin of the electron possesses additional properties that are not established by this calculation alone.

In particular, electron spin has a two-valued projection structure and exhibits fermionic transformation and exchange properties.

These characteristics cannot be inferred solely from the numerical agreement between a classical axial angular momentum and ħ/2.

The present model therefore addresses the possible electromagnetic origin of the angular-momentum scale. A complete explanation of electron spin must additionally account for its quantum structure.

The significance of the result is that a toroidal configuration with a single closed mode and three coupled field components can reproduce approximately the required axial angular-momentum value without introducing an independent angular-momentum scale into the calculation.

7.10 Conclusions

The proposed electromagnetic torus has been examined as a possible source of the electron's intrinsic angular momentum.

The E and B field components are assigned persistent mean axial contributions, while the P field participates in internal energy and momentum exchange with a vanishing mean axial contribution.

Using the energy fractions obtained from the idealized E–P–B cycle, the collective velocity associated with three equal inertial coefficients, and representative inner and outer circulation radii, the calculation gives

$$\langle J_z \rangle \approx 0.5006$$

This is close to the measured electron spin projection magnitude ħ/2.

The calculation identifies a specific relationship between the spatial energy distribution and the angular-momentum scale.

The remaining requirement is to establish the actual field-momentum distribution and its conservation throughout the complete energy-exchange cycle.

The result provides a quantitative foundation for examining the electric charge distribution and magnetic moment of the same toroidal configuration. [2], [4], [6]

8. Electric Charge and External Field

8.1 Electric Charge as an Effective Property

In conventional electrostatics, the electron is characterized by its electric charge, which determines the strength and direction of the surrounding electric field. The electric charge is represented by the quantity Q, while the spatial distribution of the electric field is described by Maxwell's equations.

The present torus model investigates a more elementary interpretation of this relationship. Instead of introducing electric charge as an independent material constituent, it examines whether the external electric field may originate from the periodic electromagnetic processes occurring within the torus.

The central proposal is that the P field periodically generates an electric field whose sign and propagation direction change during the oscillation cycle. One part of the cycle contributes to the surrounding electromagnetic field, whereas the opposite part is directed toward the interior of the toroidal cross-section.

The external field is therefore associated with the spatial and temporal superposition of periodically generated electric-field contributions.

Once a persistent external field with the required net electric flux has been established, its source can be represented by an equivalent electric charge. This equivalent charge has the same operational meaning as the charge used in conventional electrostatics, although the proposed model assigns it an underlying dynamical origin.

The objective of this section is to establish a quantitative relationship between the internal field amplitude, the temporal emission window, the geometry of the torus, and the equivalent electric charge.

8.2 Periodic Generation of the Electric Field

The preceding Part A1 introduced the coupled electromagnetic dynamics of the torus and illustrated the periodic evolution of the electric, magnetic, and P-field contributions in Figure 8.

The present analysis adopts this periodic behavior without reconstructing the detailed mechanism by which P generates E.

For a local field component, the signed electric oscillation is represented by

$$E(t) = E_0 \cos(\omega t)$$

where E_0 is the maximum electric-field amplitude and ω is the angular frequency.

The sign of E must be distinguished from its direction of propagation. The sign describes the orientation of the electric-field vector relative to a selected local reference axis, whereas the propagation direction describes the progression of the electromagnetic disturbance or associated energy flow.

In the proposed torus model, these characteristics are coupled in a specific manner.

During the negative electric-field phase, the P field generates a contribution that propagates outward from the toroidal cross-section.

During the positive phase, the generated field is directed toward the center of the cross-section. Contributions arriving from opposite regions interact with the local field generated by P.

The model proposes that this interaction suppresses the outward contribution of the positive phase. The energy associated with the inward-directed field remains involved in the subsequent E–P–B energy-exchange cycle rather than being permanently stored or destroyed.

The direction of field propagation must also be distinguished from the orientation of the electric-field vector relative to the outward normal of a closed surface. The latter determines the sign of the electric flux and therefore the equivalent electric charge.

Consequently, the two phases need not contribute equally to the external electric field.

The resulting asymmetry is the starting point for the proposed emergence of an effective electric charge.

8.3 Temporal Window of the External Field

The propagation asymmetry can be represented by a temporal window function.

Introduce the phase variable

$$\theta = \omega t$$

and a dimensionless function G(θ), which describes the fraction of the locally generated electric-field component contributing to the exterior.

The external contribution is represented by

$$E_{\text{ext}}(\theta) = E_0 G(\theta) \cos\theta$$

For an idealized transmission window,

$$0 \le G(\theta) \le 1$$

The function is zero when no contribution reaches the exterior and unity when the local component is fully transmitted.

The mean external electric field over one period is

$$\overline{E}_{\text{ext}} = \frac{E_0}{2\pi} \int_0^{2\pi} G(\theta) \cos\theta \; d\theta$$

For a window selecting a negative mean contribution, define the positive dimensionless coefficient

$$\eta = -\frac{1}{2\pi} \int_0^{2\pi} G(\theta) \cos\theta \; d\theta$$

The resulting mean field is

$$\overline{E}_{\text{ext}} = -\eta E_0$$

This equation provides a direct relationship between the amplitude of the internal Maxwell electric-field oscillation and the mean field associated with the selected outward contribution.

The coefficient η contains the effect of the temporal window. Its value depends on both the duration of the window and the shape of the electric-field oscillation within it.

For complete transmission of the negative sinusoidal half-cycle,

$$G(\theta) = 1 \quad \text{for} \quad \frac{\pi}{2} < \theta < \frac{3\pi}{2}$$

with G = 0 elsewhere, integration gives

$$\eta = \frac{1}{\pi}$$

and therefore

$$\overline{E}_{\text{ext}} = -\frac{E_0}{\pi}$$

For a narrower window corresponding to the negative quarter-cycle from π to 3π/2,

$$\eta = \frac{1}{2\pi}$$

and

$$\overline{E}_{\text{ext}} = -\frac{E_0}{2\pi}$$

These cases provide useful limiting examples. The physical transmission window must ultimately be established by the spatial interaction of the generated electric field with the P-field structure.

8.4 Superposition of Electric-Field Pulses

The torus is a continuous closed structure. Its electromagnetic oscillation is distributed around the major circumference, and different regions can contribute to the field at an external observation point with different phases and propagation delays.

The total external electric field is the vector sum of these contributions:

$$\mathbf{E}_{\text{ext}}(\mathbf{r}, t) = \sum_{i=1}^{N} \mathbf{E}_i(\mathbf{r}, t)$$

Each contribution depends on its local phase, spatial orientation, amplitude, and propagation time.

An important property of such a system is that the sum of periodically interrupted contributions can be significantly more uniform in time than the individual contributions.

To demonstrate this principle, consider equally spaced phase offsets

$$\phi_i = \frac{2\pi i}{N}$$

and identical negative half-cycle pulse functions

$$g(\theta) = \max(0, -\cos\theta)$$

In a scalar illustration in which the contributions have equal weight and the same projected direction, the total magnitude is proportional to

$$F_N(\theta) = \sum_{i=0}^{N-1} g(\theta + \phi_i)$$

For a continuous, uniformly phased distribution,

$$\lim_{N\to\infty} \frac{F_N(\theta)}{N} = \frac{1}{2\pi}\int_0^{2\pi} g(\phi)\, d\phi = \frac{1}{\pi}$$

The normalized result is independent of time.

Thus, although each local contribution is periodic, their uniformly distributed superposition can produce a constant scalar field component.

This establishes the mathematical possibility of converting a periodic sequence of contributions into a stationary aggregate.

For the physical torus, however, the contributions are vectors. Their different directions, positions, and propagation delays must be included before the same conclusion can be applied to the complete external electric field.

The continuous phase distribution around the torus can suppress temporal variations in the superposed field contributions. Whether this process produces a stationary external electric field with a nonzero net flux depends on their complete spatial and vector organization.

8.5 Effective Electric Charge and Electric Flux

The external electric field can be characterized by its flux through a closed surface surrounding the torus.

The equivalent electric charge is defined operationally by

$$Q_{\text{eff}} = \varepsilon_0 \oint_S \overline{\mathbf{E}}_{\text{ext}} \cdot d\mathbf{A}$$

Here, the overbar denotes a time average over the internal oscillation period.

This definition does not require Q_eff to be introduced as a separate material component. It characterizes the net electric flux of the resulting field.

To obtain a simple quantitative relation, consider the surface of an ideal torus with circular cross-section.

Its area is

$$A = 4\pi^2 Ra$$

Assume, as an effective boundary approximation, that the time-averaged external electric field has a uniform normal component directed inward through this surface.

The mean normal field is then

$$\overline{E}_n = -\eta E_0$$

and the corresponding equivalent charge is

$$Q_{\text{eff}} = -\varepsilon_0 A \eta E_0$$

Substituting the toroidal surface area gives

$$Q_{\text{eff}} = -4\pi^2 \varepsilon_0 Ra\eta E_0$$

This relationship follows from the assumed mean normal electric field over the toroidal surface. The temporal coefficient η determines the reduction of the oscillating field amplitude, while the spatial field configuration determines whether the resulting electric flux is nonzero. Both conditions are required for the proposed effective-charge interpretation.

This is the principal quantitative relationship of the reduced model.

It connects the equivalent charge with four structural quantities: the major radius R, the minor radius a, the electric-field amplitude E_0, and the temporal window coefficient η.

More generally, if the normal component is not uniform, the full surface integral must be retained.

The simplified formula therefore represents an effective boundary model. Its applicability depends on the spatial organization of the outward field contributions and is not implied by the temporal averaging alone.

In particular, a nonzero flux requires the corresponding field-source structure to be compatible with Gauss's law. In ordinary source-free Maxwell electrodynamics, periodic superposition by itself cannot generate a nonzero net flux through a closed surface.

The present model treats the required flux as a structural constraint on the P-generated electric field.

8.6 Determination of the Electric-Field Amplitude

The charge of the electron is experimentally known:

$$Q_e = -e = -1.602176634 \times 10^{-19}\,\text{C}$$

Rather than predicting this value independently, the present calculation uses it to determine the internal electric-field amplitude required by the proposed toroidal configuration.

Setting

$$Q_{\text{eff}} = -e$$

gives

$$E_0 = \frac{e}{4\pi^2 \varepsilon_0 Ra\eta}$$

The geometrical parameters obtained in Section 6 are

$$R = 3.153 \times 10^{-13}\,\text{m}$$

For the illustrative transverse ratio

$$a/R = 0.25$$

the minor radius is

$$a = 7.8825 \times 10^{-14}\,\text{m}$$

The corresponding toroidal surface area is approximately

$$A = 9.812 \times 10^{-25}\,\text{m}^2$$

The required magnitude of the mean normal electric field is

$$\left|\overline{E}_n\right| = \frac{e}{\varepsilon_0 A} \approx 1.84 \times 10^{16}\,\text{V/m}$$

For transmission of the complete negative sinusoidal half-cycle,

$$\eta = \frac{1}{\pi}$$

the required amplitude is

$$E_0 \approx 5.79 \times 10^{16}\ \mathrm{V/m}$$

For the narrower negative quarter-cycle,

$$\eta = \frac{1}{2\pi}$$

the amplitude becomes

$$E_0 \approx 1.16 \times 10^{17}\ \mathrm{V/m}$$

Transmission window	Window coefficient η	Required E_0 (V/m)
Negative half-cycle	1/π	5.79×10^{16}
Negative quarter-cycle	1/(2π)	1.16×10^{17}

Table 5. Electric-field amplitude required by the effective boundary model.

The calculated amplitudes are of the order of 10^{17} V/m.

The result illustrates how the electric-field amplitude depends on the temporal window. A shorter transmission interval requires a larger peak amplitude to maintain the same mean external field and equivalent charge.

The electron charge is an experimental input to this calculation. The resulting value of E_0 is therefore a model-dependent inferred amplitude, not an independent prediction of the elementary charge.

8.7 Connection with Conventional Electrostatics

The principal purpose of introducing Q_eff is to connect the microscopic torus model with the conventional macroscopic description of the electron.

If the external electric field has a nonzero negative monopole component and approaches spherical symmetry at distances much larger than the torus dimensions, its leading far-field term is

$$\overline{E}(r) \approx \frac{Q_{\mathrm{eff}}}{4\pi\varepsilon_0 r^2}\hat{r}$$

For the electron,

$$Q_{\mathrm{eff}} = -e$$

and therefore

$$\overline{E}(r) \approx -\frac{e}{4\pi\varepsilon_0 r^2}\hat{r}$$

Beyond the characteristic size of the torus, the conventional electrostatic description may then be used to determine the interaction with other charged particles.

The external observer need not resolve the internal electromagnetic cycle to describe this field. The equivalent charge summarizes the net effect of the internal structure.

The inverse-square law, however, does not follow from temporal constancy alone. It requires the appropriate nonzero monopole contribution to the spatial field.

The role of the torus model is therefore to connect the internal periodic dynamics with the existence and magnitude of that contribution.

8.8 Energy Conservation and Structural Stability

The periodic generation of an external electric field must be compatible with the long-term stability of the electron.

In the proposed model, the electric field alternates between an outward-directed phase and an inward-directed phase.

During the inward-directed phase, the electromagnetic energy remains part of the internal redistribution between E, P, and B.

The process is represented schematically by

E → P → B → P → E.

The external electric field must not be confused with continuous radiation of energy from the torus.

The electric flux is

$$\Phi_E = \oint_S \mathrm{b}E \cdot dA$$

whereas the electromagnetic energy flow through the surface is determined by

$$P_{\mathrm{EM}} = \oint_S \frac{E \times B}{\mu_0} \cdot dA$$

These are distinct physical quantities.

A stationary electron may possess a nonzero electric flux without continually radiating energy.

For a stable isolated configuration, the time-averaged net outward energy flow through a sufficiently distant closed surface must vanish:

$$\langle P_{\mathrm{EM}} \rangle = 0$$

The proposed conversion of periodic local field contributions into a persistent external configuration must therefore be distinguished from freely propagating electromagnetic radiation.

The detailed dynamical mechanism maintaining this distinction remains a requirement on the complete E–B–P model.

8.9 Interpretation and Limits of the Effective-Charge Model

The proposed model interprets electric charge as an effective property of the external electric field generated by periodic electromagnetic processes within the torus. The asymmetric transmission of electric-field contributions and their spatial superposition provide a possible mechanism for producing a persistent external field.

The temporal window coefficient η relates the internal electric-field amplitude to its mean external contribution. Combined with the toroidal geometry and an assumed normal field distribution, this leads to a quantitative relationship between the field amplitude and the equivalent electric charge.

The model does not yet independently derive the elementary charge. In particular, the generation of a nonzero electric flux requires a physical source mechanism consistent with Gauss's law. The detailed role of P in establishing this field configuration remains to be determined.

Nevertheless, the analysis establishes a quantitative connection between internal electromagnetic oscillations and the conventional description of electron charge, providing a basis for further development of the model.

8.10 Conclusions

The electric charge of the electron has been examined as a possible effective property of a periodically oscillating electromagnetic torus.

The proposed mechanism distinguishes the sign of the Maxwell electric field from the direction of its propagation. Negative field contributions are assumed to propagate outward, while positive contributions are directed toward the interior of the toroidal cross-section.

Spatially distributed, phase-shifted contributions can produce a persistent time-averaged field even though the individual field-generation processes are periodic.

Introducing a temporal transmission coefficient η gives the mean field relation

$$\overline{E}_{\mathrm{ext}} = -\eta E_0$$

Under the effective uniform-normal-field approximation, the equivalent charge is

$$Q_{\mathrm{eff}} = -4\pi^2 \varepsilon_0 R a \eta E_0$$

Using the measured electron charge and the working torus geometry gives electric-field amplitudes of approximately 5.8×10^{16} to 1.2×10^{17} V/m for the illustrative transmission windows considered.

The result does not predict the elementary charge independently. It establishes a relationship between the observed charge and the internal field amplitude required by the proposed model.

The effective-charge interpretation provides a possible conceptual connection between the periodic internal electromagnetic structure and the conventional electrostatic description of the electron.

A complete demonstration of charge emergence will require a self-consistent field solution that establishes the necessary spatial electric flux and its source while preserving energy conservation. [2], [5]

9. Magnetic Moment and Charge Distribution

9.1 Magnetic Moment as a Structural Constraint

The magnetic moment of the electron provides an additional quantitative test of the proposed electromagnetic torus.

The preceding sections introduced a fundamental toroidal mode, a collective circulation velocity, and an effective electric charge associated with the external field. The present section examines whether these properties can also account for the observed magnetic moment.

The magnitude of the electron magnetic moment is

$$|\mu_e| = 1.00115965\,\mu_B$$

where the Bohr magneton is

$$\mu_B = \frac{e\hbar}{2m_e}$$

The central requirement is to reproduce the magnetic moment using the same geometrical configuration and collective frequency developed in Sections 5–8.

The analysis distinguishes the total effective electric charge, which determines the external electric flux, from its possible circulation, which determines the magnetic moment.

9.2 Magnetic Moment of a Circulating Charge Distribution

For an electric current density distributed throughout a finite volume, the magnetic moment is

$$\mu = \frac{1}{2}\int_V \mathrm{b}r \times j\, dV$$

If the effective charge distribution rotates about the torus axis with a common angular velocity ω, its azimuthal current density is

$$j_\phi = \rho_q \omega r_\perp$$

The corresponding axial magnetic moment is

$$\mu_z = \frac{\omega}{2}\int_V \rho_q r_\perp^2\, dV$$

Here, ρ_q represents the signed effective charge density and r_{perp} denotes the distance from the axis of rotation.

For a distribution of negative charge, the magnetic moment is oppositely oriented to the corresponding positive angular velocity.

Introducing the charge-weighted mean-square radius,

$$\langle r_\perp^2 \rangle_Q = \frac{1}{Q_{\text{eff}}}\int_V \rho_q r_\perp^2\, dV$$

gives

$$\mu_z = \frac{Q_{\text{eff}}\omega}{2}\langle r_\perp^2 \rangle_Q$$

This expression assumes that an effective circulating current can be associated with the external charge of the torus. The external electric flux alone does not establish such a current; its dynamical origin remains an additional requirement of the model.

9.3 Collective Frequency and Electron Geometry

The major radius and collective velocity obtained previously are

$$R = 3.153 \times 10^{-13}\,\mathrm{m}$$

$$v_R = \sqrt{\frac{2}{3}}c$$

The corresponding angular frequency is

$$\omega = \frac{v_R}{R}$$

Using the resonance condition of Section 6 gives

$$\omega = \frac{m_e c^2}{\hbar} = 7.7634 \times 10^{20}\,\mathrm{rad/s}$$

The working cross-sectional ratio is

$$\frac{a}{R} = 0.25$$

Therefore, the inner and outer radial boundaries are

$$r_{\mathrm{in}} = 0.75R$$

$$r_{\mathrm{out}} = 1.25R$$

Numerically, the outer boundary lies at approximately 0.3941 pm.

These values establish the available geometrical range for a circulating effective charge distribution.

9.4 Effective Radius Required by the Magnetic Moment

For the electron,

$$Q_{\mathrm{eff}} = -e$$

The magnitude of the magnetic moment in the rigidly phase-locked effective-current approximation becomes

$$|\mu| = \frac{e\omega}{2}\langle r_\perp^2 \rangle_Q$$

Define an effective charge radius by

$$r_Q^2 = \langle r_\perp^2 \rangle_Q$$

The experimentally observed magnetic moment therefore requires

$$r_Q = \sqrt{\frac{2|\mu_e|}{e\omega}}$$

Substituting the Bohr magneton and the characteristic electron frequency gives

$$r_Q = \sqrt{1.00115965}\,\frac{\hbar}{m_e c}$$

Hence,

$$r_Q \approx 0.3864\,\mathrm{pm}$$

Relative to the major radius,

$$\frac{r_Q}{R} \approx 1.2255$$

This radius lies within the illustrative toroidal cross-section, close to its outer boundary.

The required location is approximately 90% of the radial distance from the centerline of the torus to its outer boundary.

The result indicates that the magnetic moment strongly constrains the effective radial distribution of the circulating charge.

9.5 Comparison of Charge Distributions

Different distributions of the same total charge produce different magnetic moments.

For a charge distribution concentrated at the major radius,

$$r_Q = R$$

the model gives

$$\frac{|\mu|}{\mu_B} = \frac{2}{3}$$

For an idealized charge distribution uniform in angle around a thin circular cross-sectional ring,

$$\langle r_\perp^2 \rangle_Q = R^2 + \frac{a^2}{2}$$

the corresponding result is

$$\frac{|\mu|}{\mu_B} = \frac{11}{16} = 0.6875$$

For a uniform charge density throughout the circular toroidal volume,

$$\langle r_{\perp}^2 \rangle_Q = R^2 + \frac{3a^2}{4}$$

the result is

$$\frac{|\mu|}{\mu_B} \approx 0.6979$$

All these distributions yield magnetic moments considerably below the observed electron value.

At the outer boundary, the same effective-current formula gives

$$\frac{|\mu_{\text{out}}|}{\mu_B} = \frac{25}{24} \approx 1.0417$$

The observed magnetic moment therefore lies within the algebraic range of the assumed toroidal geometry.

However, its reproduction requires a charge-weighted distribution concentrated near the outer region of the cross-section.

Effective charge distribution	Predicted magnitude
Concentrated at R	0.6667 μB
Uniform cross-sectional ring	0.6875 μB
Uniform toroidal volume	0.6979 μB
Concentrated at the outer boundary	1.0417 μB
Observed electron	1.00116 μB

Table 6. Dependence of the effective magnetic moment on the charge distribution.

These comparisons demonstrate that the spatial organization of the effective charge is a significant determinant of the magnetic moment.

9.6 A Two-Region Charge Approximation

To illustrate the required degree of radial concentration, divide the effective charge into an inner and an outer component.

Let the inner component circulate at

$$r_1 = 0.75R$$

and the outer component at

$$r_2 = 1.25R$$

Let f denote the fraction of the effective charge associated with the outer component.

The mean-square radius is

$$r_Q^2 = (1-f)r_1^2 + fr_2^2$$

Solving for f gives

$$f = \frac{r_Q^2 - r_1^2}{r_2^2 - r_1^2}$$

Using the electron magnetic-moment reference gives

$$f \approx 0.939$$

Thus, approximately 94% of the effective charge would have to be associated with the outer component in this simplified two-region approximation.

This result illustrates the strong radial asymmetry required by the model.

It is not an independently derived charge distribution. The actual spatial weighting must follow from the relationship between the P-generated external electric field and the internal circulating current.

9.7 Physical Meaning of the Circulation Velocity

The magnetic-moment calculation relates the effective circulating charge distribution to the collective angular frequency of the torus.

For the Bohr magneton, the required effective circulation radius corresponds to the reduced Compton wavelength of the electron. At this radius, the tangential phase velocity equals c.

The measured electron magnetic moment exceeds the Bohr magneton by approximately 0.116%. Reproducing this additional contribution through the same rigid-rotation

approximation would require a slightly larger effective radius and a corresponding phase velocity exceeding c.

The collective phase velocity must therefore be distinguished from the physical transport velocity of electric charge or energy. The present approximation establishes the characteristic scale of the magnetic moment, while the anomalous contribution and the detailed effective-current dynamics remain subjects for further investigation.

9.8 Relationship Between Magnetic Moment and Angular Momentum

Section 7 obtained an illustrative mean axial angular momentum of approximately

$$\langle J_z \rangle \approx 0.5006$$

The present effective-current calculation can reproduce a magnetic-moment magnitude close to μB when the charge distribution is sufficiently concentrated toward the outer region.

These results use the same major radius and angular frequency, which is an important geometrical consistency condition.

The angular momentum and magnetic moment are nevertheless generated by different model-dependent distributions.

Angular momentum depends on the complete field-momentum circulation, whereas the magnetic moment depends on the effective current density.

A complete dynamical solution must determine both distributions from the same fields rather than choosing them independently.

Numerical agreement with the electron's spin projection and magnetic moment is therefore a useful consistency test, but does not alone establish the observed electron gyromagnetic factor or the quantum nature of its spin.

9.9 Conclusions

The magnetic moment of the electron has been examined using the collective angular frequency and toroidal geometry developed in the preceding sections.

For the working geometry with R approximately 0.3153 pm and a/R = 0.25, the measured electron magnetic moment corresponds to a charge-weighted root-mean-square circulation radius of approximately 0.3864 pm.

This radius lies near the outer boundary of the proposed toroidal cross-section.

Uniform charge distributions yield magnetic moments below the electron value, while a distribution strongly concentrated toward the outer region can reproduce the required magnitude within the effective-current approximation.

The result provides a quantitative geometrical constraint on the relationship between the external effective charge and the internal electromagnetic circulation.

The remaining task is to derive the effective current distribution from the E–B–P dynamics and establish its consistency with angular-momentum conservation and physically admissible transport velocities.

The analysis therefore identifies both a promising geometrical relationship and the dynamical conditions that a complete electromagnetic model of the electron must satisfy. [1], [4], [6]

10. Structural Stability and Saturation

10.1 Stability of the Electromagnetic Torus

The electron is characterized by exceptional stability. Its rest energy, electric charge, spin, and magnetic moment remain unchanged during ordinary interactions. An electromagnetic torus proposed as a structural model of the electron must therefore possess

mechanisms that preserve its internal organization over time.

In the present model, stability is not associated with the absence of motion. The torus contains continuously oscillating electric, magnetic, and P fields, accompanied by periodic energy and momentum exchange.

The central requirement is that these internal processes form a coherent, self-maintaining configuration rather than producing progressive deformation or loss of energy.

The stability problem consequently involves three interconnected conditions: geometrical equilibrium, dynamical phase coherence, and conservation of the complete field energy.

The mechanisms responsible for these conditions were introduced in Parts A1 and A2. The present section examines their combined consequences for the energy-saturated torus identified as a possible electron structure.

10.2 Balance Between Expansion and Binding

The electric and magnetic components of the torus are associated with different structural tendencies.

The electric field contributes to the stresses that can promote geometrical expansion. The magnetic field contributes to the binding organization of the structure and opposes unrestricted expansion.

In the proposed energy interpretation, the magnetic contribution is assigned a negative binding role, while the electric energy contribution is positive.

The distinction concerns the structural energy balance. The conventional Maxwell electromagnetic energy densities remain non-negative.

For a stable binding-dominated configuration, the proposed signed internal balance satisfies

$$W_{\text{struct}} = W_E + W_{\text{binding}} + W_{P,\text{struct}}$$

where the magnetic binding contribution is negative.

This signed structural balance must be distinguished from the non-negative total physical energy used in Section 6 to represent the electron rest energy.

The stability of the torus depends not only on the magnitude of the binding contribution but also on its response to geometrical deformation. A stable configuration requires the combined electric, magnetic, and P-field stresses to produce restoring tendencies when the torus departs from its equilibrium geometry.

The equilibrium state is therefore characterized by a balance of the complete internal field stresses rather than by the comparison of two integrated energy contributions alone.

10.3 The Role of P-Field Inertia

The P field contributes an independent inertial response to the electromagnetic dynamics.

During the internal sequence

E → P → B → P → E,

P participates in the transfer of energy between the electric and magnetic configurations.

Its inertia allows the internal motion to remain continuous when either E or B passes through an instantaneous minimum.

The resulting dynamical response also influences the collective circulation around the major circumference.

In the simplified strong-coupling model developed in Section 5, three comparable inertial coefficients produce the limiting collective velocity

$$v_R = \sqrt{\frac{2}{3}}c$$

The significance of this result for stability is that the three fields can participate in a common mode rather than behaving as unrelated oscillators.

Nevertheless, a common propagation mode alone does not establish stability. The coupling must also prevent relative perturbations from growing and destroying the phase relationships required by the internal energy-exchange cycle.

The inertial role of P is therefore both to modify the collective motion and to contribute to the dynamical continuity of the toroidal structure.

10.4 Saturation and the Fundamental Mode

The electron is assumed to correspond to an energy-saturated torus in its fundamental closed mode:

n=1

The fundamental mode contains one complete phase cycle around the major circumference.

Higher-order modes are geometrically possible, but the model proposes that structural evolution favors the fundamental configuration because it minimizes unnecessary internal phase variation and permits a highly coherent organization.

During the formation and interaction of electromagnetic toruses, changes in total energy may be accompanied by changes in geometry and internal mode structure, as discussed in Part A2.

Saturation represents the state in which further structural evolution becomes strongly constrained by the balance of internal fields.

The major radius, transverse dimensions, and phase relationships must then remain mutually compatible.

The saturated configuration is not necessarily the state of greatest possible electromagnetic energy. Rather, it is a state in which the existing energy and internal geometry permit a persistent, dynamically coherent structure.

The preference for n = 1 and the existence of a saturation boundary are working hypotheses. Their rigorous justification requires comparison of the stability of different allowed modes.

10.5 Response to Geometrical Perturbations

A stable torus must resist small changes in its dimensions.

Let the major and minor radii undergo small perturbations:

$$R(t) = R_0 + \delta R(t)$$

$$a(t) = a_0 + \delta a(t)$$

The response depends on how these perturbations modify the electric, magnetic, and P-field contributions.

A simplified description can be based on a constrained effective structural-energy function

$$U = U(R, a)$$

where the relevant conserved quantities and field configuration are included in the definition of U.

The effective structural-energy function U describes the restoring response to geometrical perturbations and should not automatically be identified with the signed internal energy balance introduced in Section 10.2.

At equilibrium,

$$\left.\frac{\partial U}{\partial R}\right|_0 = 0$$

$$\left.\frac{\partial U}{\partial a}\right|_0 = 0$$

The second-order variation is

$$\delta^2 U = \frac{1}{2} K_{RR} (\delta R)^2 + K_{Ra} \delta R \delta a + \frac{1}{2} K_{aa} (\delta a)^2$$

Here, the coefficients describe the local structural stiffness around the equilibrium configuration.

For a strictly stable local minimum within this two-coordinate approximation, the conditions are

$$K_{RR} > 0$$

$$K_{RR}K_{aa} - K_{Ra}^2 > 0$$

Under these conditions, sufficiently small geometrical displacements increase the effective structural energy and experience restoring tendencies.

The actual stiffness coefficients must be obtained from the coupled electromagnetic stresses and P-field response. They have not been determined quantitatively in the present reduced model.

These conditions therefore establish the mathematical requirements for stability rather than demonstrating that the proposed torus already satisfies them.

10.6 Phase Coherence and Resonance

The torus must maintain coherence between the internal E–P–B energy-exchange cycle and the collective circulation around the major circumference.

Let Ω denote the internal energy-exchange frequency and ω the collective angular frequency.

For the simplest phase-locked configuration, the proposed resonance condition is

$$\Omega = \omega$$

The collective frequency is related to the major radius by

$$\omega = \frac{v_R}{R}$$

The period and geometric scale developed in Section 6 follow from identifying this circulation frequency with the characteristic frequency associated with the electron rest energy.

A perturbation of the torus may temporarily alter its field distribution, geometry, or relative phase.

A stable configuration requires such deviations to remain bounded and, where irreversible relaxation is possible, to return toward the original coherent state.

The existence of a common frequency is therefore an important structural condition, but it must be accompanied by suitable restoring dynamics.

The three-field model of Section 5 possesses real normal-mode frequencies for positive coupling. This supports oscillatory linear behavior within that approximation, although it does not establish complete nonlinear stability.

10.7 Radiation and Conservation of Energy

The stable electron does not continuously radiate away its rest energy.

The proposed torus must therefore maintain a non-radiating stationary configuration even though its internal electromagnetic fields undergo periodic changes.

The electromagnetic energy flow is described by the Poynting vector

$$S = \frac{1}{\mu_0} E \times B$$

For an isolated stable configuration, the time-averaged outward energy flow through a sufficiently distant closed surface must vanish:

$$\left\langle \oint_S \mathrm{b}S \cdot dA \right\rangle = 0$$

Internal circulation and redistribution of energy do not necessarily imply a net outward energy loss.

Likewise, a persistent external electric field does not itself require continuous radiation.

However, periodic internal motion can radiate if its associated electromagnetic multipole moments vary in a manner that produces outgoing waves.

The toroidal geometry and phase coherence are proposed to suppress such radiation in the stationary state.

A complete demonstration must establish the cancellation or absence of the relevant outgoing radiation fields.

The non-radiating character of the saturated torus is therefore an essential stability requirement rather than an automatic consequence of geometrical closure.

10.8 Stability During External Interactions

The structural stability of the electron must also persist during ordinary interactions with other particles and electromagnetic fields.

Small external disturbances may temporarily modify the geometry, internal field amplitudes, or phase relationships of the torus. If the stable configuration possesses suitable restoring dynamics, these changes need not destroy its identity.

Interactions between two electron toruses provide a simple example. Their external electric fields produce Coulomb repulsion, so noncentral encounters generally result in deflected trajectories rather than direct overlap of the internal structures. In a head-on encounter, the repulsive field reduces their approach velocity and can reverse their relative motion before strong structural overlap occurs. At sufficiently high interaction energies, the internal response would require a more detailed dynamical calculation. Thus, external electric repulsion can reduce the occurrence of strong overlap, while the internal field balance remains responsible for the stability of each individual torus.

10.9 The Saturated Torus as an Electron Candidate

The preceding analysis identifies the fundamental saturated torus as a candidate stable electromagnetic structure. Its stability is associated with the combined effects of electromagnetic binding, P-field inertia, geometrical equilibrium, and phase coherence.

The significance of this configuration lies in its ability to connect structural stability with the same internal dynamics used to investigate the electron's energy, angular momentum, electric charge, and magnetic moment.

A complete stability demonstration requires the restoring forces, nonlinear field response, and radiation properties to be established quantitatively. The present model nevertheless provides a unified framework for examining these requirements within a single electromagnetic structure.

10.10 Conclusions

The stability of the proposed electron torus is associated with the combined action of electromagnetic binding, P-field inertia, geometrical equilibrium, and phase coherence.

The fundamental mode n = 1 and the energy-saturated configuration provide the structural basis for persistent closed motion.

Small perturbations must generate restoring responses, while the internal electromagnetic dynamics must conserve energy and avoid continuous radiation.

The analysis identifies the physical and mathematical conditions required for a stable toroidal electron model.

These conditions provide the foundation for a unified quantitative comparison with the measured properties of the electron in the following section. [6], [7], [8]

11. Quantitative Comparison with the Electron

11.1 Purpose of the Quantitative Comparison

The preceding sections developed an electromagnetic torus model based on three mutually coupled field components, E, B, and P. The model combines closed toroidal geometry, periodic internal energy exchange, collective field inertia, and an effective external electric charge.

The purpose of the present section is to compare the quantitative consequences of this structure with the experimentally established properties of the electron.

A central requirement is that the different electron properties be associated with one coherent toroidal configuration. The model should not require an independently selected radius, oscillation frequency, or propagation velocity for every observed quantity.

Three categories of quantities are distinguished in this comparison.

The first consists of experimentally measured electron properties used as reference values or input constraints.

The second consists of quantities calculated from the assumed toroidal geometry and simplified field dynamics.

The third consists of model parameters or distributions whose values remain to be determined from a complete solution of the coupled field equations.

This distinction makes it possible to evaluate the quantitative consistency of the proposed model without confusing a fitted parameter with an independent physical prediction.

11.2 Fundamental Parameters of the Electron

The experimentally established properties relevant to the present analysis are summarized in Table 7.

The rest energy defines the characteristic angular frequency

$$\omega_e = \frac{m_e c^2}{\hbar}$$

and the corresponding reference period

$$T_e = \frac{h}{m_e c^2}$$

Physical quantity	Reference value
Rest mass	9.10938×10^{-31} kg
Rest energy	0.510999 MeV
Electric charge	$-1.602176634 \times 10^{-19}$ C
Spin quantum number	1/2
Spin projection magnitude	ħ/2
Magnetic moment magnitude	1.00115965 μB
Electron g-factor magnitude	2.00231930
Characteristic period from rest energy	8.0933 zs
Reduced Compton wavelength	0.386159 pm

Table 7. Electron properties used as quantitative reference values.

These quantities establish an energy-related frequency scale. The identification of this scale with the circulation period of the torus is an assumption of the proposed structural model.

The measured electric charge and magnetic moment provide additional constraints on the external field and its possible effective current distribution.

11.3 Calculated Geometry and Collective Motion

The proposed electron torus is associated with the fundamental closed mode

n=1

For three equal characteristic inertial coefficients and strong coupling, Section 5 obtained the collective phase velocity

$$v_R = \sqrt{\frac{2}{3}}c \approx 0.8165c$$

Identifying one collective circulation with the characteristic electron period gives

$$R = \frac{v_R}{c}\frac{\hbar}{m_e c}$$

and consequently

$$R \approx 0.3153\,\mathrm{pm}$$

The result connects the collective field inertia with the geometrical scale of the proposed electron structure.

For the illustrative transverse ratio

$$\beta = \frac{a}{R} = 0.25$$

the minor radius becomes

$$a \approx 0.0788\,\mathrm{pm}$$

The inner and outer radial boundaries are approximately 0.2365 pm and 0.3941 pm, respectively.

The numerical values are summarized in Table 8.

Parameter	Calculated or assumed value	Basis
Fundamental mode n	1	Structural hypothesis
Collective velocity	0.8165c	Strong-coupling approximation
Circulation period	8.0933 zs	Matched to electron energy
Major radius R	0.3153 pm	Calculated from period and velocity
Ratio a/R	0.25	Illustrative geometrical assumption
Minor radius a	0.0788 pm	Calculated from assumed ratio
Total energy	0.510999 MeV	Electron rest-energy constraint

Table 8. Geometrical and dynamical parameters of the working torus model.

The collective velocity follows from the simplified three-field equations, whereas the major radius is fixed by matching the calculated circulation period to the reference period derived from the measured electron mass.

Thus, the calculation establishes a geometrical relationship rather than an independent prediction of electron mass.

11.4 Angular Momentum

Section 7 examined the mean axial angular momentum arising from the effective circulation of the E and B field-energy contributions.

The idealized energy-exchange model of Section 4 gives the time-averaged fractions

$$\frac{\langle W_E\rangle}{W_0} = \frac{3}{8}, \qquad \frac{\langle W_B\rangle}{W_0} = \frac{3}{8}, \qquad \frac{\langle W_P\rangle}{W_0} = \frac{1}{4}$$

The P field was assumed to have a vanishing mean axial angular-momentum contribution.

Using illustrative effective circulation radii

$$r_E = 0.75R, \qquad r_B = 1.20R$$

the reduced model gives

$$\frac{\langle J_z\rangle}{\hbar} = \frac{3}{8}\left(\frac{v_R}{c}\right)^2 (0.75^2 + 1.20^2)$$

For the strong-coupling collective velocity,

$$\langle J_z\rangle = 0.500625$$

The electron spin projection magnitude is

$$|S_z| = 0.500000$$

The relative numerical difference is approximately 0.125%.

This close agreement is noteworthy because the mean energy fractions were obtained from

the idealized energy-exchange cycle rather than adjusted to reproduce the spin value.

However, the characteristic radial positions of the E and B contributions remain illustrative assumptions.

Furthermore, the reduced energy-circulation expression has not yet been derived from the complete electromagnetic momentum density and P-field dynamics.

The result therefore demonstrates that the required axial angular-momentum scale is attainable within the selected geometrical approximation.

The stationary torus is assumed to conserve its total angular momentum despite the periodic redistribution of energy between E, B, and P. A complete description must establish the underlying field-momentum distribution and account for the quantum properties of electron spin.

11.5 Electric Charge and External Field

Section 8 investigated the electric charge as a possible effective property of the periodically generated external electromagnetic field.

The proposed mechanism distinguishes between the negative electric-field phase, which contributes to the surrounding space, and the positive phase, which is directed toward the interior of the toroidal cross-section.

The temporal window is represented by the coefficient

$$\eta = -\frac{1}{2\pi}\int_0^{2\pi} G(\theta)\cos\theta \; d$$

For an idealized uniform normal-field distribution over the toroidal surface, the corresponding effective charge is

$$Q_{\text{eff}} = -4\pi^2\varepsilon_0 Ra\eta E_0$$

The observed electron charge is used to determine the necessary electric-field amplitude:

$$E_0 = \frac{e}{4\pi^2\varepsilon_0 Ra\eta}$$

For the working torus geometry, the resulting amplitudes are approximately

$$E_0 = 5.79 \times 10^{16}\ \text{V/m}$$

for transmission of the negative half-cycle, and

$$E_0 = 1.16 \times 10^{17}\ \text{V/m}$$

for the selected negative quarter-cycle.

These are inferred amplitudes calculated from the measured electron charge.

The time-window model establishes the relationship between the electric-field amplitude and its temporal average. The additional uniform-normal-field assumption establishes the corresponding effective flux relationship.

A complete derivation of the electron charge must still demonstrate that the physical E–B–P dynamics generate the required nonzero electric flux.

Consequently, the present result is a quantitative calibration of the external-field model, not an independent prediction of the elementary charge.

11.6 Magnetic Moment and Charge Distribution

Section 9 examined whether the same torus geometry and collective angular frequency can reproduce the observed electron magnetic moment.

In the effective circulating-current approximation,

$$|\mu| = \frac{e\omega}{2}\langle r_\perp^2\rangle_Q$$

The required charge-weighted root-mean-square radius is

$$r_Q = \sqrt{\frac{2|\mu_e|}{e\omega}}$$

Using the measured magnetic moment and the collective frequency determined in Section 6 gives

$$r_Q \approx 0.3864\,\mathrm{pm}$$

This radius lies within the assumed toroidal cross-section, whose outer radial boundary is approximately 0.3941 pm.

The result indicates that the observed magnetic moment is compatible with the available geometrical range of the model, provided that the effective circulating charge is strongly weighted toward the outer region.

By contrast, uniform effective charge distributions yield smaller magnetic moments.

A distribution concentrated at the major radius gives approximately 0.6667 μB, while a uniform toroidal volume distribution gives approximately 0.6979 μB.

The observed value of 1.00115965 μB therefore requires a substantial outward displacement of the charge-weighted effective radius.

The calculation is subject to two important conditions.

The observed magnetic moment requires an effective current distribution concentrated toward the outer region of the toroidal cross-section. This result provides a quantitative constraint on the spatial organization of the effective charge within the geometry established in Section 6.

The calculation reproduces the characteristic scale of the Bohr magneton. The measured anomalous contribution and the detailed physical relationship between the effective charge and its circulating current remain to be established from the coupled field dynamics.

11.7 Combined Quantitative Assessment

The principal results can now be compared within a single table.

Electron property	Experimental reference	Torus-model result	Interpretation
Rest energy	0.511 MeV	0.511 MeV	Input constraint
Characteristic period	8.0933 zs	8.0933 zs	Imposed resonance condition
Collective velocity	No directly measured internal value	0.8165c	Approximate dynamical result
Major radius	No established measured electron radius	0.3153 pm	Conditional geometrical result
Spin projection magnitude	0.5000 ħ	0.5006 ħ	Conditional geometrical consistency
Electric charge	−e	−e	Calibration input
Electric-field amplitude E_0	No independent measured internal value	Approximately 10^{17} V/m	Inferred from charge
Magnetic moment	1.00116 μB	Matched with outer-weighted distribution	Model-dependent fit
Structural stability	Stable electron	Proposed restoring mechanisms	Not yet quantitatively demonstrated

Table 9. Quantitative comparison between the electron and the electromagnetic torus model.

The comparison reveals several relationships.

First, the three-field inertial model provides a definite collective phase velocity and, when combined with the electron reference period, a characteristic toroidal radius.

Second, the energy distribution and spatial field-circulation model can reproduce an axial

angular-momentum value close to the electron spin projection.

Third, the effective-charge model connects the measured electron charge with an inferred internal electric-field amplitude and the duration of the external-field window.

Fourth, the magnetic-moment calculation places a strong constraint on the radial distribution of the effective circulating charge.

These results establish a connected quantitative framework.

However, the model has not yet obtained all electron properties as independent predictions from one complete solution of the field equations.

The principal remaining requirement is to derive the spatial energy, momentum, and effective-current distributions self-consistently from the coupled E–B–P dynamics.

11.8 Conclusions

The quantitative comparison demonstrates that several fundamental electron properties can be examined within a common electromagnetic torus geometry and a unified framework of coupled E–B–P dynamics.

The simplified model establishes relationships between collective field inertia, characteristic period, toroidal dimensions, angular momentum, effective electric charge, and magnetic moment. The resulting numerical consistency provides a basis for further development of the proposed electron structure.

The principal remaining task is to derive the required spatial field distributions and their dynamical stability from a common set of equations, allowing the electron properties to emerge as interconnected consequences of the same electromagnetic configuration.

12. Discussion

The results presented in this article suggest that an electromagnetic torus may provide a common structural framework for several fundamental properties of the electron. Rather than treating mass, angular momentum, electric charge, and magnetic moment as unrelated characteristics, the proposed model connects them with the geometry and internal dynamics of a single coherent electromagnetic configuration.

A central feature of the model is the interaction between the three coupled fields E, B, and P. The P field introduces an additional inertial response and participates in the periodic exchange of energy between the electric and magnetic components. This provides a physical basis for collective motion at a velocity different from that of a freely propagating electromagnetic wave.

The fundamental closed mode, n = 1, connects the internal oscillation with the toroidal geometry. By relating its circulation period to the characteristic period associated with the electron rest energy, the model establishes a definite geometrical scale. The same configuration permits quantitative estimates of angular momentum and magnetic moment, illustrating the importance of the spatial distributions of field energy and effective current.

A particularly significant aspect is the interpretation of electric charge as an effective property of the external electric field rather than an independent material constituent. The proposed asymmetry between outward- and inward-directed field contributions offers a mechanism for producing a persistent average external field. Establishing a nonzero net electric flux, however, requires a consistent description of the P-generated field compatible with Maxwell's equations.

The stability of the proposed electron structure is associated with electromagnetic binding, P-field inertia, phase coherence, and geometrical

saturation. The mechanisms developed in Parts A1 and A2 provide the foundation for this interpretation, while Part A3 examines their consequences for the fundamental saturated state.

The principal contribution of the model is a unified physical picture in which several electron properties are connected to one organized electromagnetic structure. The quantitative results provide a basis for further development, particularly the derivation of the spatial field distributions, effective currents, and stability conditions from a common set of dynamical equations.

13. Conclusions

This article has developed a structural model of the electron based on an energy-saturated electromagnetic torus. The proposed configuration combines three dynamically coupled fields, E, B, and P, whose periodic interaction provides a common physical framework for investigating the fundamental properties of the electron.

The introduction of P as an independent inertial component connects internal electromagnetic energy exchange with collective motion and the characteristic geometry of the torus. The quantitative analysis demonstrates that the proposed structure can approach the electron's axial angular momentum and accommodate its magnetic moment through suitable spatial distributions of electromagnetic energy and effective current.

A significant conceptual result is the interpretation of electric charge as an effective property of the external electric field generated by internal electromagnetic processes. This approach connects the periodic field dynamics of the torus with the conventional electrostatic description, while identifying the conditions required for a complete derivation of the external electric flux.

The stability of the saturated torus is associated with electromagnetic binding, P-field inertia, phase coherence, and geometrical equilibrium. Together, these mechanisms provide a basis for investigating a persistent electromagnetic structure capable of maintaining its identity as a particle.

The results establish a coherent conceptual and quantitative framework for further development. The central contribution of Part A3 is the possibility of interpreting several fundamental electron properties as interconnected manifestations of a single organized electromagnetic structure, supporting the broader investigation of electromagnetic toruses as possible fundamental constituents of matter.

References

[1] Mohr, P. J., Newell, D. B., Taylor, B. N., and Tiesinga, E. (2025). CODATA recommended values of the fundamental physical constants: 2022. *Reviews of Modern Physics*, 97, 025002. https://doi.org/10.1103/RevModPhys.97.025002

[2] Jackson, J. D. (1998). *Classical Electrodynamics* (3rd ed.). John Wiley & Sons.

[3] Landau, L. D., and Lifshitz, E. M. (1975). *The Classical Theory of Fields* (4th ed.). Pergamon Press.

[4] Schwinger, J. (1948). On Quantum-Electrodynamics and the Magnetic Moment of the Electron. *Physical Review*, 73, 416–417. https://doi.org/10.1103/PhysRev.73.416

[5] Dubovik, V. M., and Tugushev, V. V. (1990). Toroid moments in electrodynamics and solid-state physics. *Physics Reports*, 187(4), 145–202. https://doi.org/10.1016/0370-1573(90)90042-Z

[6] Radescu, E. E., and Vaman, G. (2002). Exact calculation of the angular momentum loss, recoil force, and radiation intensity for an arbitrary source in terms of electric, magnetic, and toroid multipoles. *Physical Review E*, 65, 046609. https://doi.org/10.1103/PhysRevE.65.046609

[7] Rozman, F. *Part A1 – Electromagnetic Torus: Internal Field Structure and Stability*. Manuscript, Unified Electromagnetic Theory of Matter and Light.

[8] Rozman, F. *Part A2 – Merging and Structural Evolution of Electromagnetic Tori*. Manuscript, Unified Electromagnetic Theory of Matter and Light.